DEPARTMENT OF PHYSICS
THE UNIVERSITY OF
ARIZONA

Naval Air Systems Command

(15) N00019-78-C-0479

(6) Determination of optical constants for powdered materials in the 10 micron infrared region.

(9) Final Report,

(11) 3 Sep 79

Principal Investigator:

(10) Donald R. Huffman
Department of Physics
University of Arizona
Tucson, Arizona 85721

401 873

(12) 62

September 3, 1979

401 873

I. INTRODUCTION

With the increasing importance in modern warfare of infrared laser weaponry, guidance systems, and thermal imaging devices, it has become more and more important that we understand techniques for obscuration by particulate systems, i.e. smoke screens. A light beam is attenuated by the two processes, absorption and scattering, the sum of these being called extinction. A desirable property of the screening smoke is high extinction efficiency per unit volume or per unit mass of the material (depending on the exact application). In order to attenuate CO_2 laser radiation one requires a particulate system having large extinction coinciding with the CO_2 laser emission band wavelengths of approximately 9.6 and/or 10.6 μm. Band widths need not be large in this case. For the purpose of screening against thermal imaging devices, which may utilize the entire atmospheric window region between about 8 and 14 μm wavelength, a considerably wider particulate extinction band is called for. One might at first think that the best approach would be to use an aerosol which would give high extinction throughout the infrared. It is possible, however, to achieve much higher extinction in a narrow band than in a wide band, as will be shown in this report.

A. Purpose of this work

In order to successfully tailor the aerosol to the specific need we should be able to engineer the optical properties of the particulates, that is to calculate the performance of various systems and to produce the one that most closely fits the desired characteristics. In order to accomplish this optical engineering of aerosols the following two things are necessary:

(1) A catalogue of the wavelength-dependent optical

constants for various solids and liquids.

(2) Adequate theoretical representation of how extinction is related to such factors as particle size, shape, and coating.

Great difficulties have been present in both of these areas. Regarding the all important optical constants, there is no extensive compilation available. This is true in spite of the fact that there is a large amount of literature on certain optical characteristics such as transmission. Optical constants, however, are usually determined only for homogeneous samples such as single crystals and bulk liquids. Unfortunately, most solids have not been produced as single crystals, but are commonly available only in powdered form. A technique to permit accurate determination of optical constants for powdered materials would provide a much needed means for filling this gap in our basic physical data bank. The main goal of this work has been to attempt development of such a technique.

In the course of the technique development we have had to deal critically with point (2) above, the theory of small particle extinction. Some progress in the theoretical treatment of shape effects has been achieved as a necessary part of the optical constants technique development. The purpose of this report is to describe the development of the technique for determining optical constants of powdered solids and to summarize the procedure. Application of the method to four solids with well-known optical constants provides a means for evaluating the success of the procedure. As a by-product, some insights we have gained into the larger question of how to produce maximum extinction will be discussed.

B. Organization of this report

Organization of this report will be in the following way. In part II we discuss methods for determining optical

constants starting with the well-tested methods used on smooth, bulk materials. This enables us to present a viewpoint on how to treat the similar but much more difficult problem in powdered samples. Difficulties in previous attempts at determining optical constants for powders are discussed, and the philosophy of the present work is presented, emphasizing the special need for better understanding of absorption by irregularly shaped particles. In part III we point out why it is desirable to limit both experiments and theory to the Rayleigh regime. Part IV develops a theory for treating irregular shapes which, while not perfect, gives a significant improvement over the theory for spheres. Part V summarizes the experimental techniques for measuring extinction by small particles and compares the measurements with calculations based on the shape distribution theory of IV for the cases of four solids with well-known optical properties. Part VI presents our attempts to invert the small particle extinction data for the four "known" solids and discusses the degree of success. The larger question of how does one produce maximum extinction by means of absorption by particles in the 10 μm spectral region is returned to in part VII Several insights into this question gleaned from the present combination of theory and experiment are commented on. Finally part VIII summarizes the conclusions of this work and makes suggestions for further work.

II. DISCUSSION OF SOME METHODS FOR DETERMINING OPTICAL CONSTANTS

The basic optical properties of matter, such as absorption, reflection, and scattering, are determined by the wavelength-dependent complex optical constants

$$m(\lambda) = n + ik$$

where n is the index of refraction and k is the extinction

coefficient (although this terminology will be avoided in this report because of possible confusion with small particle extinction). There are numerous common misconceptions concerning optical constants, such as that n must be greater than one to avoid violation of Einsteinian relativity -- not true; such as that n may be considered as approximately constant as k varies -- not always true. These misconceptions, both of which play a part in this discussion, probably arise because technical people have been trained by their elementary optics teaching that n is essentially constant ($\simeq$1.5) with only a small dispersion toward the blue that increases n by a few percent, while k is usually zero but may vary a little in colored materials. These statements are, after all, true for glasses in the visible, which is what traditional optics is all about. The truth is, however, that in the more remote wavelength regions of the ultraviolet and the infrared all solids have regions in which both n and k vary over wide ranges. Very commonly n is less than 1, k is greater than n, and both vary over orders of magnitude within a narrow wavelength region. Examples of this behavior will come up in this report.

In addition to the indices of refraction, optical properties can be summarized in terms of complex dielectric functions

$$\varepsilon(\lambda) = \varepsilon_1 + i\varepsilon_2 \quad .$$

The complex indices of refraction and the complex dielectric functions are directly related in the following way:

$$\begin{aligned} \varepsilon_1 &= n^2 - k^2 \\ \varepsilon_2 &= 2nk \end{aligned} \qquad (1)$$

Hence either pair of quantities can be said to completely describe the optical properties of a substance, and we shall frequently use the term optical constants to refer to either set.

A. Bulk optical constants

The most direct determination of optical constants is accomplished by measurement of transmission through a slab of the material and reflectance from its surface. For wavelength regions and for solids of concern in this work, however, absorption in so great that bulk solids cannot be produced in sufficiently thin slices that any measured light can penetrate through the slab. One must necessarily resort to pure reflectance techniques. Since, however, one measurement cannot determine the two desired quantities, the usual procedure is to measure reflectance under two different conditions (two polarization states at non-normal incidence or two different angles) or to measure reflectance over an extended wavelength range coupled with an analysis that properly relates n and k. It is this last technique that we shall present.

The normal incidence reflectance R of a surface of material characterized by optical constants n and k is given by the Fresnel equation

$$R = \frac{(n-1)^2 + k^2}{(n+1)^2 + k^2} \qquad (2)$$

where the material is assumed to be in air with index of refraction taken to be 1. When the reflectance of certain solids is measured in the infrared there is a region of wavelengths for which R is very close to 1. An example is shown in the a part of figure (1) for the solid silicon carbide. The historical terminology for the highly reflecting region is "reststrahlen" region, since multiple reflection of polychromatic light from such a solid results in "residual radiation" at these wavelengths. The reststrahlen region is caused by strong interaction of light with the ionic vibration modes of the crystal. Almost all solids and liquids have vibrational

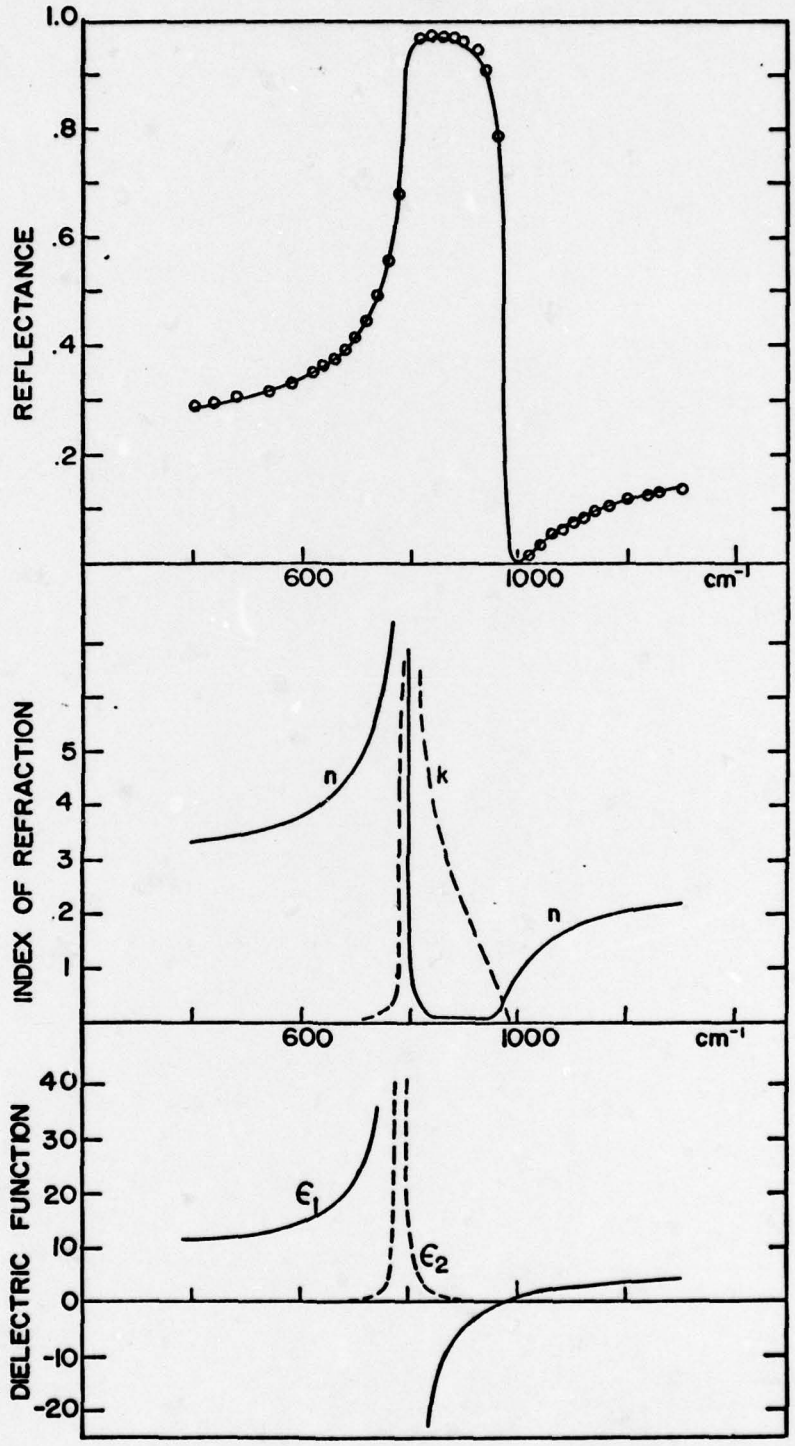

Figure 1: (a) Measured reflectance, (b) derived optical constants, and (c) derived dielectric functions for α-SiC from Spitzer, Kleinman, and Walsh (1959). The circles in the reflectance graph represent some of the data points and the continuous curves in all three graphs are calculated from the one oscillator fit to the data with

$$\varepsilon_0 = 6.7 \quad \omega_0 = 793 \quad \omega_p = 1443 \quad \gamma = 4.76 \ .$$

absorption bands in the infrared, but the strengths of the bands may not be great enough to produce a reflectance approaching 1 as in the reststrahlen case. It is, however, the strong vibrational interaction that ultimately gives rise to the strong small particle absorption bands that are of chief concern in this work. Hence our attention is focused primarily on bands such as those of figure (1a). For such cases it has been found that a charged harmonic oscillator model of the crystal vibrations and their interaction with the electromagnetic field gives a quite accurate description of the optical effects in the bulk solid. For a solid composed of N identical oscillators per unit volume the complex dielectric function is (Hodgson 1970, for example)

$$\varepsilon = \varepsilon_\infty + \frac{\omega_p^2}{\omega_0^2 - \omega^2 + i\gamma\omega} \qquad (3)$$

where $\omega_p^2 = Ne^2/m$ is the plasma frequency of the ions of mass m. ω_0 is the vibrational frequency related to the effective spring constant and the mass, and γ is the damping factor. ε_∞ is the dielectric function at high frequencies compared to the oscillator frequency. The high frequency dielectric constant is normally due to the effect of electronic oscillators in the ultraviolet. If there are several types of oscillators, due for example to different bonds between ions, equation (3) can be written as a sum over the several types j,

$$\varepsilon = \varepsilon_\infty + \sum_j \frac{\omega_{p,j}^2}{\omega_j^2 - \omega^2 + i\gamma_j\omega} \qquad (4)$$

The multiple oscillator model forms the basis of a common

technique for analyzing normal incidence reflectance data for bulk optical constants of the solid. The results are illustrated in figure (1) for the solid silicon carbide. Values of the parameters $\varepsilon_0, \gamma, \omega_0$ and ω_p are assumed (guessed) and used in equation (3) to calculate $\varepsilon_1(\lambda)$ and $\varepsilon_2(\lambda)$, which are converted to $n(\lambda)$ and $k(\lambda)$ using equations (1). Indices of refraction are then used in equation (2) to calculate $R(\lambda)$. The parameters are varied until the calculated reflectance gives a good match to the measured reflectance spectrum. Once the fit is achieved the oscillator parameters then give $\varepsilon_1(\lambda)$ and $\varepsilon_2(\lambda)$ or $n(\lambda)$ and $k(\lambda)$ as desired. The full curves in figure (1a) are the calculated values as compared with measured reflectance values denoted by circles. Optical constants in (1b) and (1c) are the inferred values based on the best fit.

If the solid is anisotropic the technique can still be employed provided the sample is cut and oriented properly and polarized light is used. A classic example of optical constants determination for an anisotropic solid using the multiple oscillator expression (4) is the work on crystalline quartz of Spitzer and Kleinman (1961). Figure (2) shows the measured reflectance for the two major crystalline directions as solid lines and the fits to the data achieved using the multiple oscillator theory. Their derived parameters and the optical constants resulting from them will by used in our work discussed later in this report.

There are several reasons for our presenting these details of the technique for determining optical constants by using the oscillator model. We will use an analogous method in our task of determining n and k for powdered materials. Secondly, we wish to assure the reader that the oscillator model, although very simple, has convincing validity when applied to solids such as we are most interested in. Finally, this commonly used method for "measuring" optical constants emphasizes the necessity of interposing theory (in this case

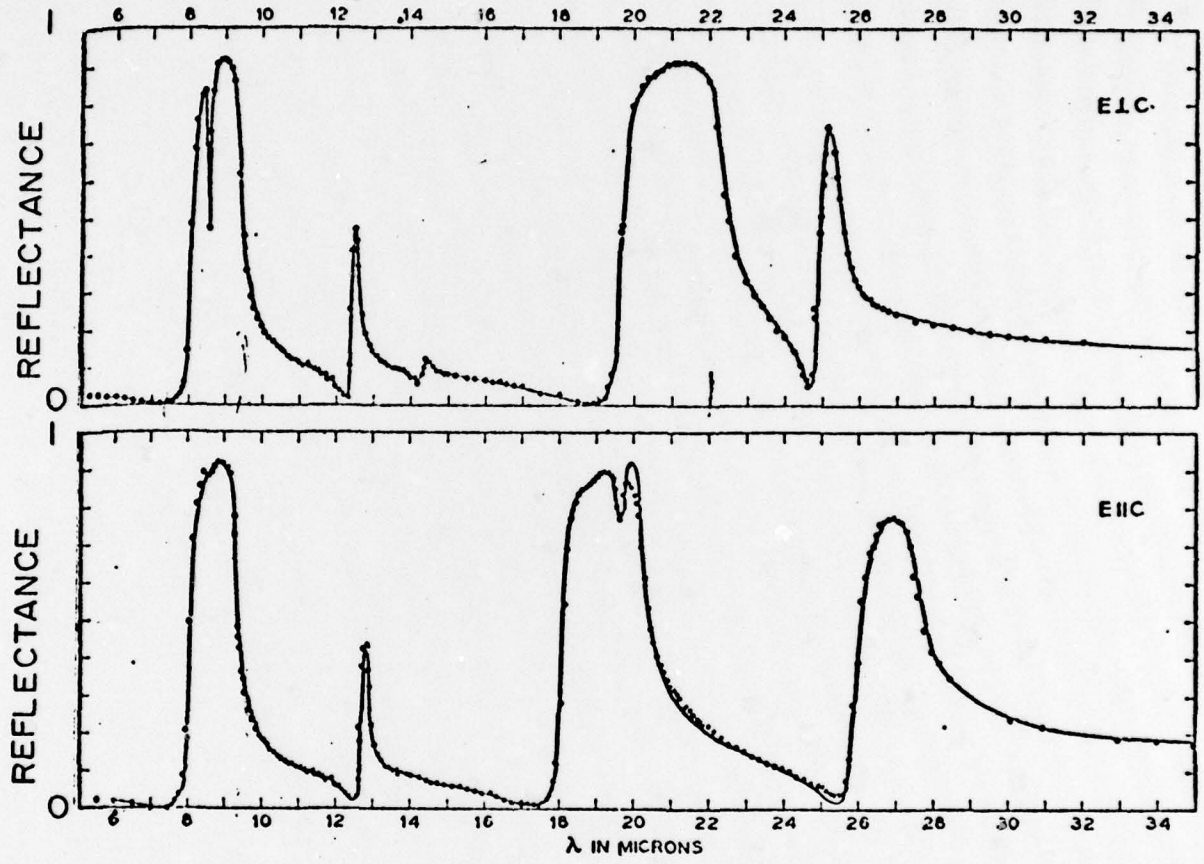

Figure 2 Reflectivity of oriented single crystal quartz for the two major polarization directions. Data are shown by the points and the theoretical fit by the solid lines.

Lorentz oscillator theory plus Fresnel's equation) between the measurements and the derived quantities. Diagramatically,

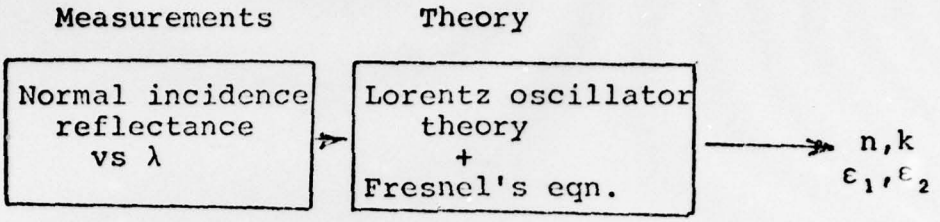

Another popular technique of analyzing normal incidence reflectance data for extracting optical constants is by means of so-called Kramers-Kronig relations. This technique has been discussed in many places (see for example Stern 1964). The diagram is

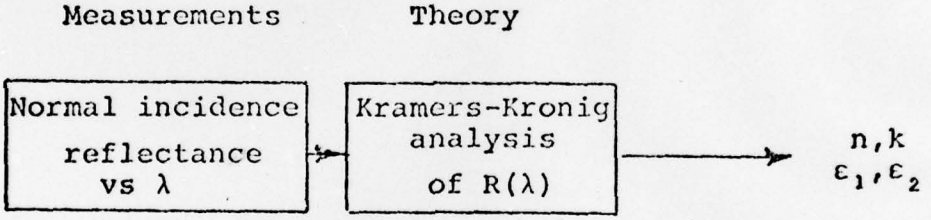

It is frequently true, as in the above situations, that the quantity "measured" is actually an inferred quantity based on the actual measurement of a related quantity coupled with some sort of connecting link, the theory. Assuming that the measurements are perfectly correct, the results can still be accurate only if the intermediary theory is accurate and applies accurately to the experimental situation. In the case of the above mentioned determinations of optical constants for quartz and for SiC, we have great confidence in Fresnel's equations, the Kramers-Kronig relations, and the Lorentz oscillator equations. Furthermore, single crystals such as were used in these examples can be cleaved or polished to insure that the

normal incidence reflection equation is accurately obeyed in the experimental measurements.

A more subtle feature of the two bulk optical constants methods is that n and k are correctly related to one another. It is an important point in this work that n and k (or ε_1 and ε_2) are not independent quantities but are real and imaginary parts of the same complex quantities. As such they are inseparably related to one another. The relationship of ε_1 and ε_2 to one another can be expressed in fact by another one of the Kramers-Kronig relations.

$$\varepsilon_1(\omega) = 1 + \frac{2}{\pi} \int \frac{\varepsilon_2(\omega')\omega'}{\omega'^2 - \omega^2} d\omega' \qquad (5)$$

$$\varepsilon_2(\omega) = \frac{2}{\pi} \int \frac{\omega\varepsilon_1(\omega')}{\omega'^2 - \omega} d\omega'$$

Any method that determines a wavelength-dependent ε_1 (or n) by one technique and a wavelength dependent ε_2 (or k) by an unrelated technique that does not properly acknowledge the inter-relationship of the quantities should be used with caution.

B. Small particle optical constants

Several attempts have been made to determing optical constants of powdered or otherwise inhomogeneous materials. Volz (1972), for example, has presented "measured" optical constants for atmospheric dust particles, Perry et. al. (1972) have given optical constants for lunar soil samples, and Penman (1976a,b) has inferred optical constants from minerals and meteoritic material bearing a possible relation to interstellar grains. The subject of our present study is (fortunately) a little simpler than most of these tasks. We are

dealing with only one chemical component, such as SiC or $CaCO_3$, in powdered form, as opposed to a rock, a lunar soil sample, a collection of atmospheric dust, or a meteorite, each of which are multicomponent mixtures. Some of the work by Volz and some by Penman were concerned with single component powders, however, and will be discussed briefly. A recent paper by Jennings et. al. (1979) has been critical of the techniques for determining optical constants of inhomogeneous materials, particularly for atmospheric particulates. We now discuss some of the difficulties in relation to previous methods of determining optical constants and to our own proposed method. Our conclusions are that, despite difficulties, there is hope of extracting reasonably reliable optical constants from one-component, powdered materials. The discussion of difficulties emphasizes experimental and theoretical problems to which particular attention must be paid.

The method which Volz (1972) has used for atmospheric particulates is summarized in our diagrammatic way as follows:

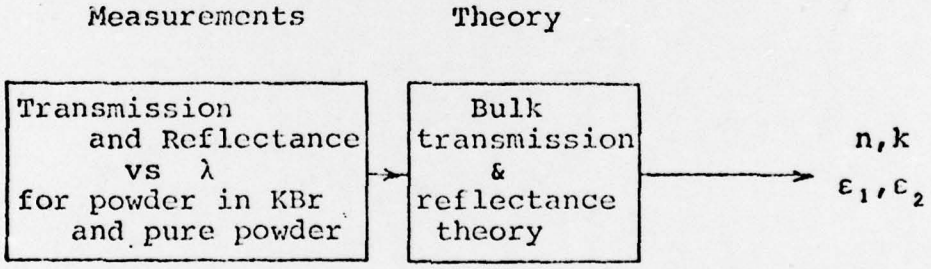

Volz mixed a small quantity of sample powder into KBr, formed a pellet and measured transmission. The transmission (T) was analyzed using the equation

$$T = \exp\left(-\frac{4\pi k}{\lambda} t\right) \qquad (6)$$

where λ is the wavelength and t is the effective thickness of

the sample powder. This equation treats the sample powder as a homogeneous slab. The procedure has been justly criticized by Jennings et. al. for not taking into account certain small particle properties such as scattering and the size dependence of extinction. Volz continues his determination of n by using the k's derived from equation (6) along with measured normal incidence reflectance R of compressed powder (with no KBr) in equation (2). In many cases powders cannot be compressed to anything like bulk solid surfaces so that the bulk reflectance equation is not applicable. Even if (6) were perfectly applicable and if there were no scattering effects and size dependence of extinction, the serious errors introduced by treating extinction as a bulk property in determining k would carry over to introduce serious errors in n.

We have tried Volz's method in an attempt to derive optical constants of MgO. Ther results were so far off that no purpose seemed to be served by showing them. The reason for the severe difficulty in this technique as applied to solids with strong infrared bands is as follows. Small particles of a solid have resonant absorption modes at different wavelength than does the bulk solid, but this does not imply that the optical constants of the small particle and the bulk are different. The shift in absorption bands is perfectly calculable from bulk optical constants. For spheres the small particle mode occurs at the wavelength for which $\varepsilon_1 = -2\varepsilon_m$. ε_m is the dielectric function for the surrounding medium, in this case KBr. The bulk solid has its resonant mode at the frequency where ε_2 is a maximum. Thus if equation (6) is employed, treating the small particles as bulk, the inferred ε_2 (or k) is substantially displaced from its true position. Introduction of this highly erroneous k into the reflectance equation then gives rise to even worse values of n. Without desiring to be critical we have mentioned this technique to emphasize the errors that can accrue when proper account is not taken of small particle

as opposed to bulk properties.

Penman's (1976) approach has been to measure specular reflectance at almost-normal-incidence for his heterogeneous solids and to analyze by means of the Fresnel reflectance equation (2) and Kramers-Kronig analysis, as though the sample were a homogeneous solid with a smooth, plane surface.

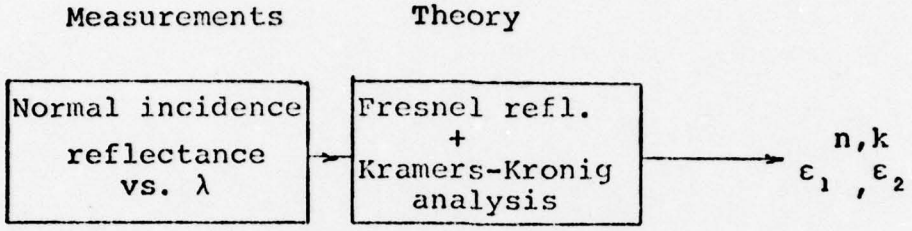

This is the exact technique that has been used often for bulk solids, but the theory is not strictly applicable to the inhomogeneous samples, and the effect of optical anisotropy is not taken into account.

The approach we outlined in the proposal for this contract was to use transmission measurements of the particulates as a dilute suspension in a KBr pellet, similar to what Volz did. We proposed to analyze the transmission measurements by using small particle absorption and scattering theory coupled with a multiple oscillator theory.

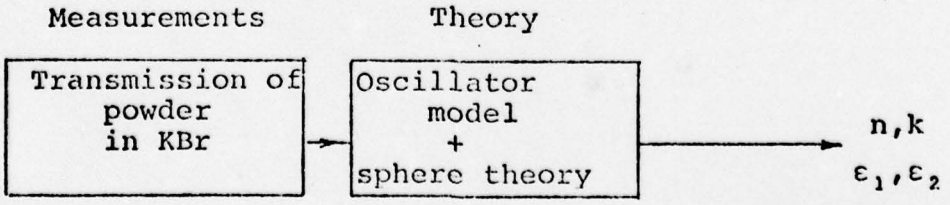

The merit of this approach as contrasted with the Volz and Penman approaches is that it takes into account specifically the small particle nature of the sample. Optical constants

are also related correctly to one another in a self consistent way by the oscillator model. Unfortunately, our early work under this contract proved that a very important factor is not included in this approach -- the shape distribution of the particles.

Although it is commonly believed that shape effects are not important in the Rayleigh region, especially for absorption, this is not at all true in the vicinity of very strong infrared resonances. A preview of figure (7), which will be discussed in more detail later, will show the reader that the sphere theory using accurately measured bulk optical constants of quartz fails badly in calculating the extinction band properties of a real powder of quartz particles. The discrepancy lies in the fact that absorption modes in individual particles are quite shape dependent. Because of the inadequacy of sphere theory in regard to shape effects we have made considerable effort in attempting to develop a theory to correctly treat irregular shapes. This extensive digression was not planned at the beginning of the work but turned out to be a necessary deviation from the original plan. Having developed a more successful small particle theory for treating shape effects, discussed in part III, our method for inferring optical constants now has become

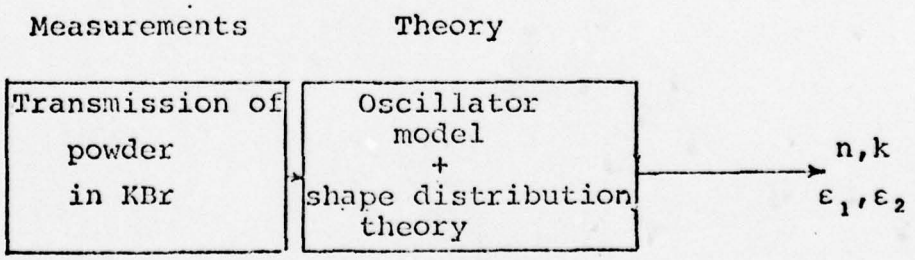

We have given the preceeding discussion in order to emphasize that one does not measure optical constants directly; one performs related measurements that are analyzed with

the help of appropriate theory to infer n and k. The weakest part of the process for small particles seems to be the theory box. It is difficult to make the experiment exactly conform to the theory (perfectly isolated spherical particles, for example), and it is difficult to construct a theory that correctly interprets the actual experiment (somewhat clumpy collections of highly irregular particles). The game we play is a difficult one, and the results can hardly be expected to be as accurate as single crystal results.

III. LIMITATION OF THEORY AND EXPERIMENT TO THE RAYLEIGH REGION

Although the difficulties in inverting experimental measurements on powders to obtain optical constants are severe, great simplifications occur if only particles are considered that are small enough for the Rayleigh approximation to be valid. The conditions for applicability of the Rayleigh approximation are that the particle dimensions (l) are small compared to the wavelength (λ) and that the phase shift, $2\pi ml/\lambda$, across the particle is small. The important simplifications resulting from use of the Rayleigh theory are the following:

(1) there are no size effects in volume-normalized extinction.

(2) shape effects, which are substantial in work of this sort, can be simply treated theoretically.

In this section we will demonstrate with sphere calculations how the size dependence goes away for small radii, then show how inadequate is the spherical theory even in the small particle limit. Finally, we preview the results from section IV by showing the improvement a Rayleigh theory of shape distribution can provide over the spherical theory.

A. Size dependence

The only shapes of arbitrarily large particles for which an exact solution to the electromagnetic boundary value problem is possible are spheres (the Mie theory) and infinitely long cylinders. By using Mie theory (see van de Hulst 1957, for example) it is possible to determine how the extinction coefficient, normalized per unit volume of solid, varies as the particle size (radius) changes. Figure (3) shows results (Day et. al. 1974) of Mie calculations based on measured optical constants at infrared wavelengths where maximum absorption occurs in the vicinity of 10 μm. Three silicate materials were chosen for which the absorption strengths are quite large. One sees that at small radii (less than 0.5 μm) the volume normalized extinction is constant. For radii greater than about 1 μm the extinction is extremely size dependent, falling quickly as radius increases. This decrease of extinction with radius is a saturation phenomenon which occurs when absorption is so effective that the inner parts of the sphere are hardly influenced by the electromagnetic fields. As the radius increases, the volume increases, but more and more of the inner volume is ineffective; thus the absorption per unit volume decreases. For particles in the 1 to 10 μm size range it should be clear that the exact size distribution must be known and taken into account in order to infer optical constants from measured extinction. For particles smaller than about 0.8 μm, however, figure (3) shows that the size distribution is immaterial since extinction per unit volume has become independent of size. This is the consideration demanding that we experimentally select out the sub-micron size fraction, if at all possible, for doing our extinction measurements on. Jennings et. al. (1979) have called attention to the size dependence problem in analyzing optical measurements of powders and have pointed out the necessity of knowing the size distribution. We circumvent the

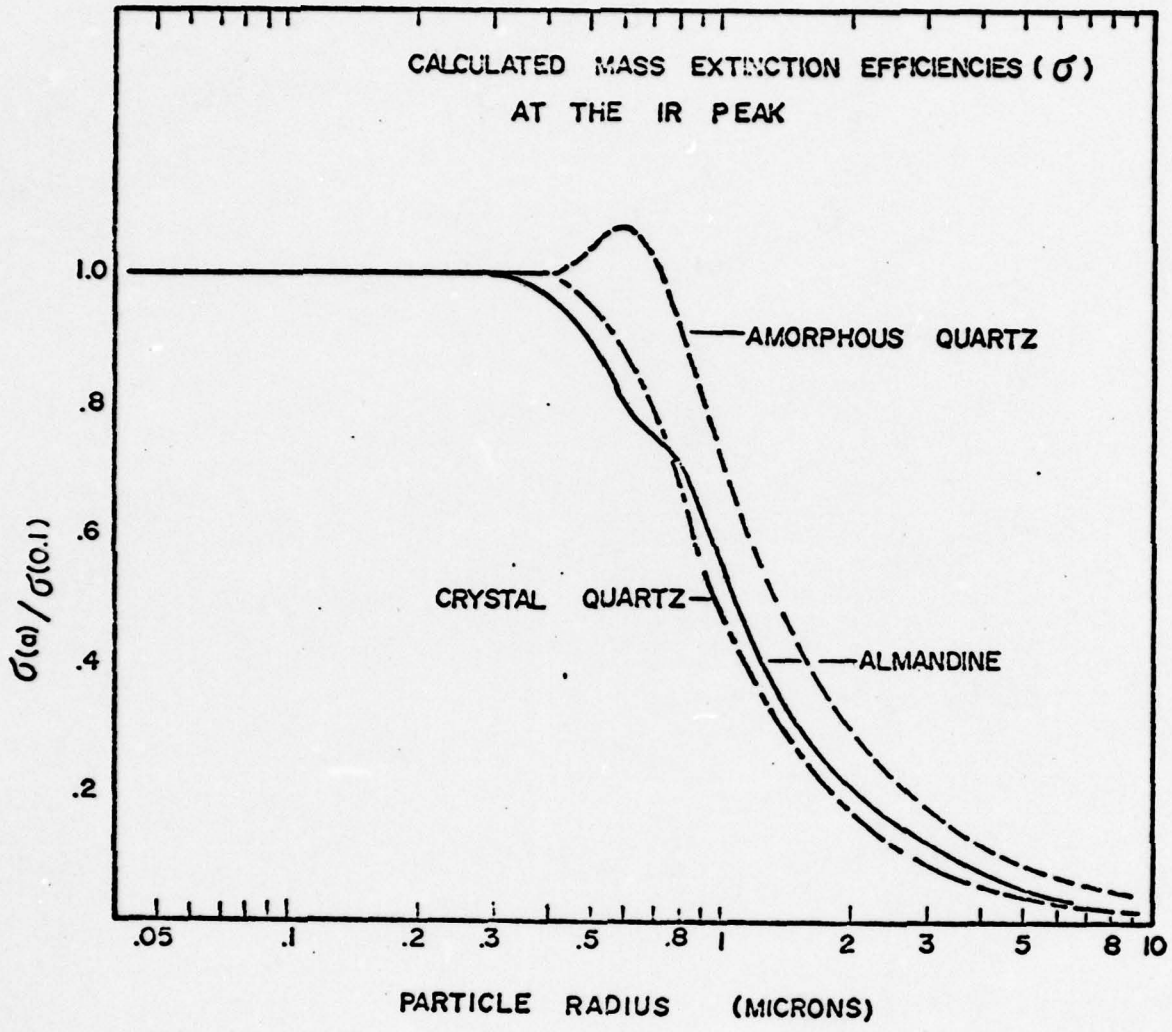

Figure 3

Peak mass extinction coefficient (σ) vs. particle radius (a) for amorphous quartz, as well as crystalline quartz and almandine, normalized to unity for spheres with radii equal to 0.1μ.
(from Day, et. al., 1974)

need for knowing the size distribution by selecting only particles small enough for the size distribution to be immaterial.

In order to confirm the size dependence and to develop techniques for selecting a suitably small size fraction we have segregated a powder of quartz into several size fractions by differential settling in water. Stokes' law for the rate of settling of spherical particles of radius r with density ρ_1 falling in a medium with density ρ_2 and viscosity η is

$$v = \frac{2}{9} \frac{(\rho_1 - \rho_2)}{\eta} gr^2 \qquad (7)$$

where g is the acceleration due to gravity. For quartz falling in water the velocity is given by

$$v = 3.6 \times 10^{-4} r^2$$

where v is in cm/sec and r is in μm. Therefore the radius of a particle can be determined if the distance traveled and the time are measured. Experimentally, approximately 10 grams of a finely ground quartz powder were mixed with 5 - 10 ml of distilled water. A 100 ml graduated cylinder whose height was marked in cm's was filled nearly to the top with distilled water. The dense quartz suspension was poured into the cylinder and allowed to settle for a predetermined length of time, after which successive portions of the fluid were drawn off from the top and placed in petri dishes. The water was then allowed to evaporate, leaving behind "sized" particles.

Extinction measurements were made for a few different sized particle fractions of the quartz encapsulated in KBr pellets. (See section V for a more detailed description of the sample preparation and measurement techniques.) Transmission curves for three of the size fractions in KBr are shown in figures 4,5, and 6. Figure 4 for the large size fraction also shows a light micrograph of the particles, con-

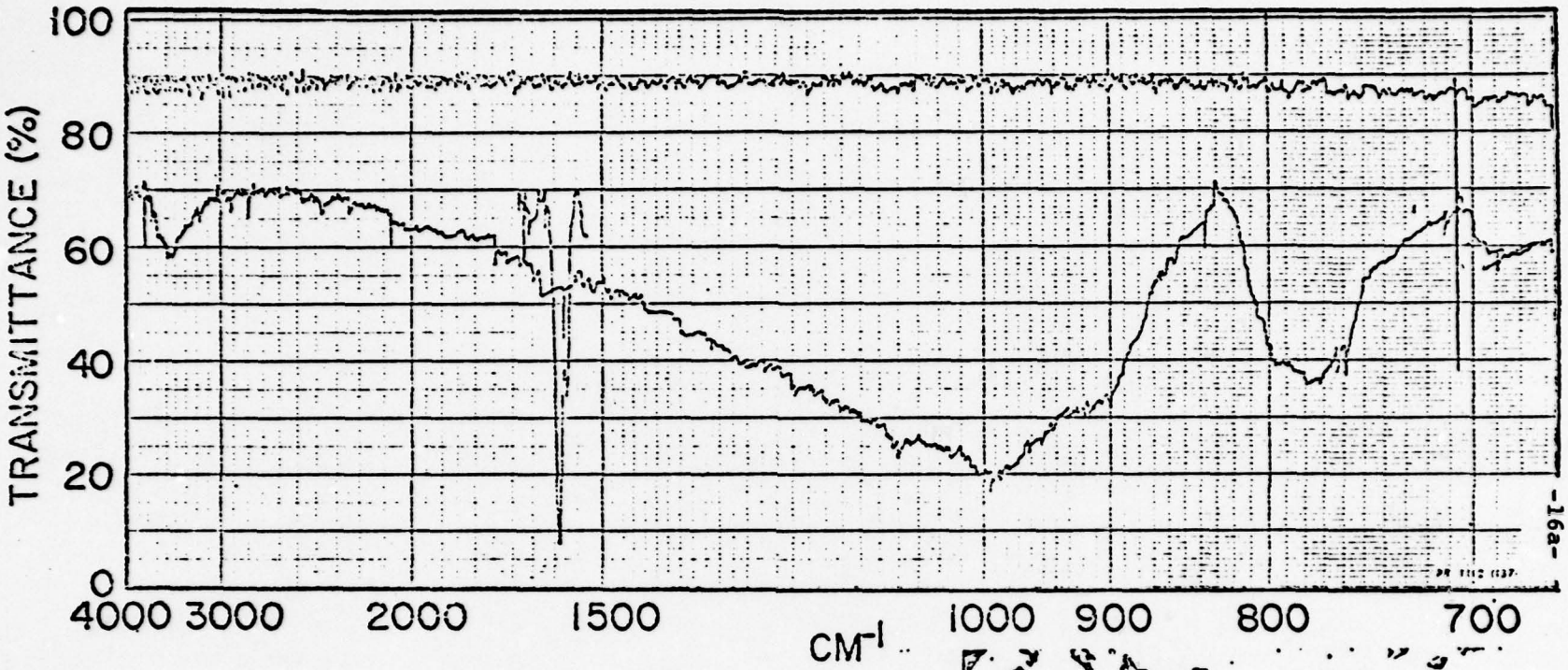

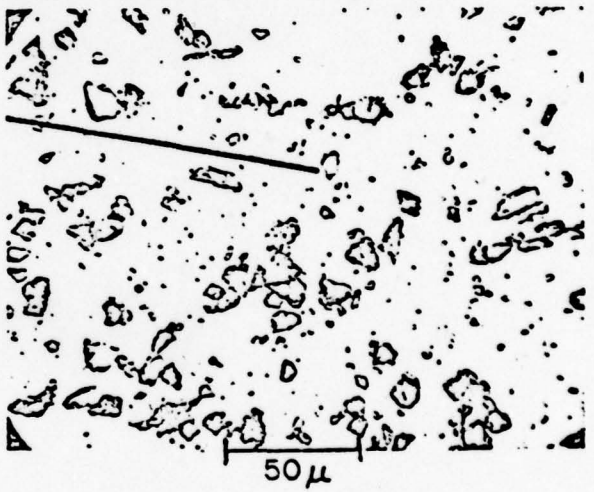

Figure 4

Extinction vs. frequency for fused silica particles with $5.2\mu < r < 6.7\mu$. Also shown is a light micrograph of the particles.

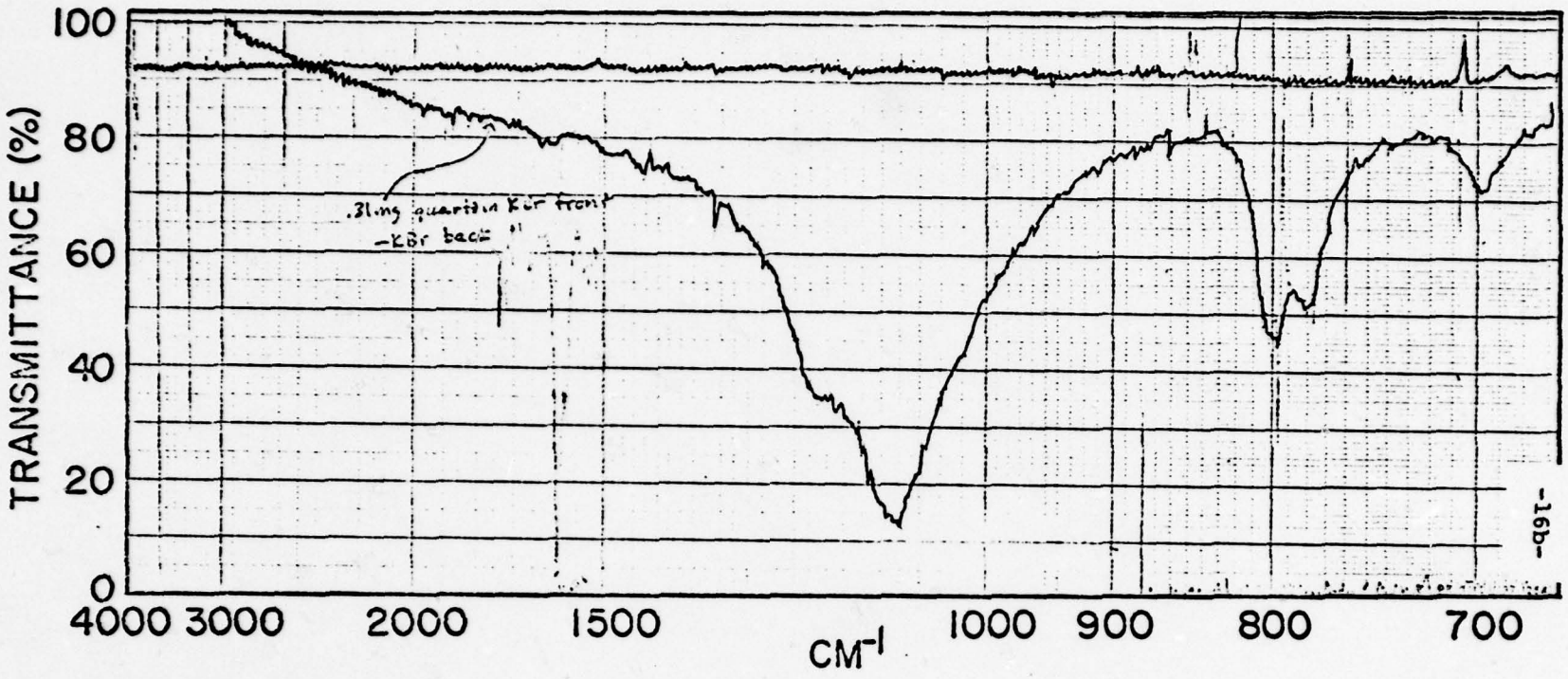

Figure 5

Extinction vs. frequency for fused silica particles with r≤2μ.

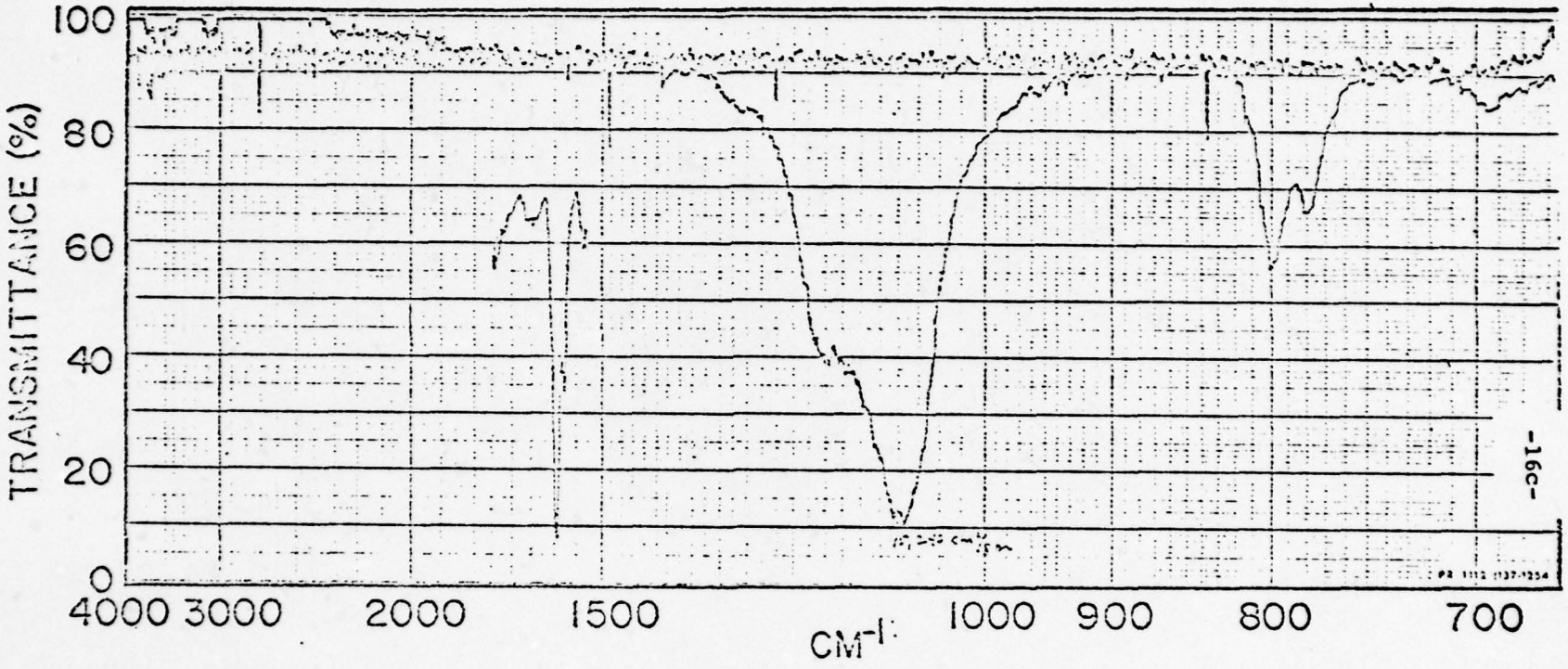

Figure 6

Extinction vs. frequency for fused silica particles with $0.8\mu < r < 1.1\mu$.

firming that they are indeed quite irregularly shaped. Comparison of the three spectra including the derived mass-normalized extinction coefficients at the peak shows that the shape of the extinction spectrum for large particles is quite different from the spectrum of the smaller particles. The peak mass extinction coefficient decreases markedly in going to the smaller sizes, in agreement with the discussion of figure (3). Table I summarizes the peak mass extinction coefficients for the several size fractions of quartz.

TABLE I

Mass normalized extinction coefficients for quartz particles in KBr

Size range (μm)	Peak position (cm^{-1})	Mass extinction coeff. (cm^2/g)
$5.2 < r < 6.7$	1000	1,300
$r < 2$	1086	8,000
$0.8 < r < 1.1$	1084	15,400
$r < 0.8$	1087	33,100

The implications of these results are clear. To avoid the messy and complex problem of dealing with extinction varying in a complicated way with size distribution one should experimentally separate out a size fraction for which this problem does not exist. Our experiments on quartz particle segregation have convinced us that this is possible. The technique has therefore been adopted as standard practice.

B. Shape effects

Having eliminated the size dependence problem our next

concern was to compare measurements with the theory for spheres. In this case and in the rest of our work, absolute normalization of the extinction coefficient by unit volume (rather than by unit mass) has been used. It is important for us to point out that we are not making any arbitrary scaling of either the experiment or the theory, as is very frequently done in such comparisons. Figure (7) shows the volume-normalized extinction coefficient determined experimentally from the small size fraction of quartz powder, compared with the calculated extinction based on accurately measured bulk optical constants for quartz (Spitzer and Kleinman 1961). The agreement is seen to be very poor. Maximum extinction shows a disagreement of more than a factor of five, and widths and shapes of the strong extinction band compare poorly. The problem is evidently shape effects. We have used a theory for spheres to apply to highly irregular particles (see inset of figure 4). Our theory block of section II is not wrong, but it is inappropriate to the measurement block. It is evident that use of the sphere theory to invert the measurements for optical constants would likely lead to very bad results. One needs either to create spheres of the particles or to construct a theory capable of a better representation of irregular particles. Since it appears impractical for us to make spheres (less than 1μm in diameter) of all solids we wish to study, our alternative has been to attempt development of a more satisfactory theoretical treatment. Fortunately, for particles of this size range, the Rayleigh theory is a rather good approximation, and shape effects can be easily treated, to some extent, by considering ellipsoids with a wide variation of axial ratios. Details of this development are given in the next section. In the lower curves of figure (8) we preview our theoretical results for quartz (one of the better cases). Results of extinction from the distribution of Rayleigh ellipsoids calculation are compared with the measured extinction curve, with no arbitrary scaling. It is

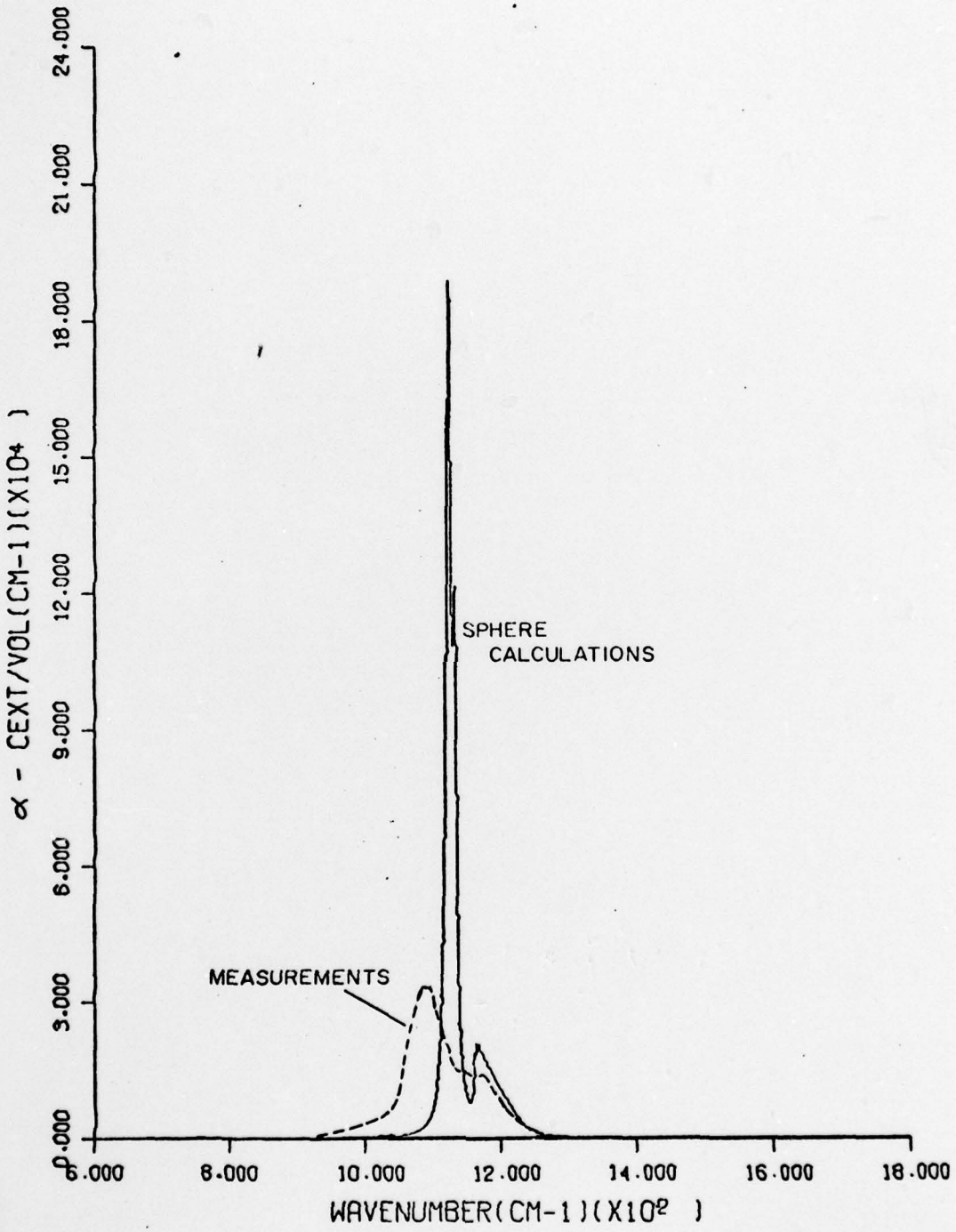

Figure 7: Comparison of extinction calculated for spherical particles of quartz in KBr with measured extinction for a small size fraction of quartz powder in KBr.

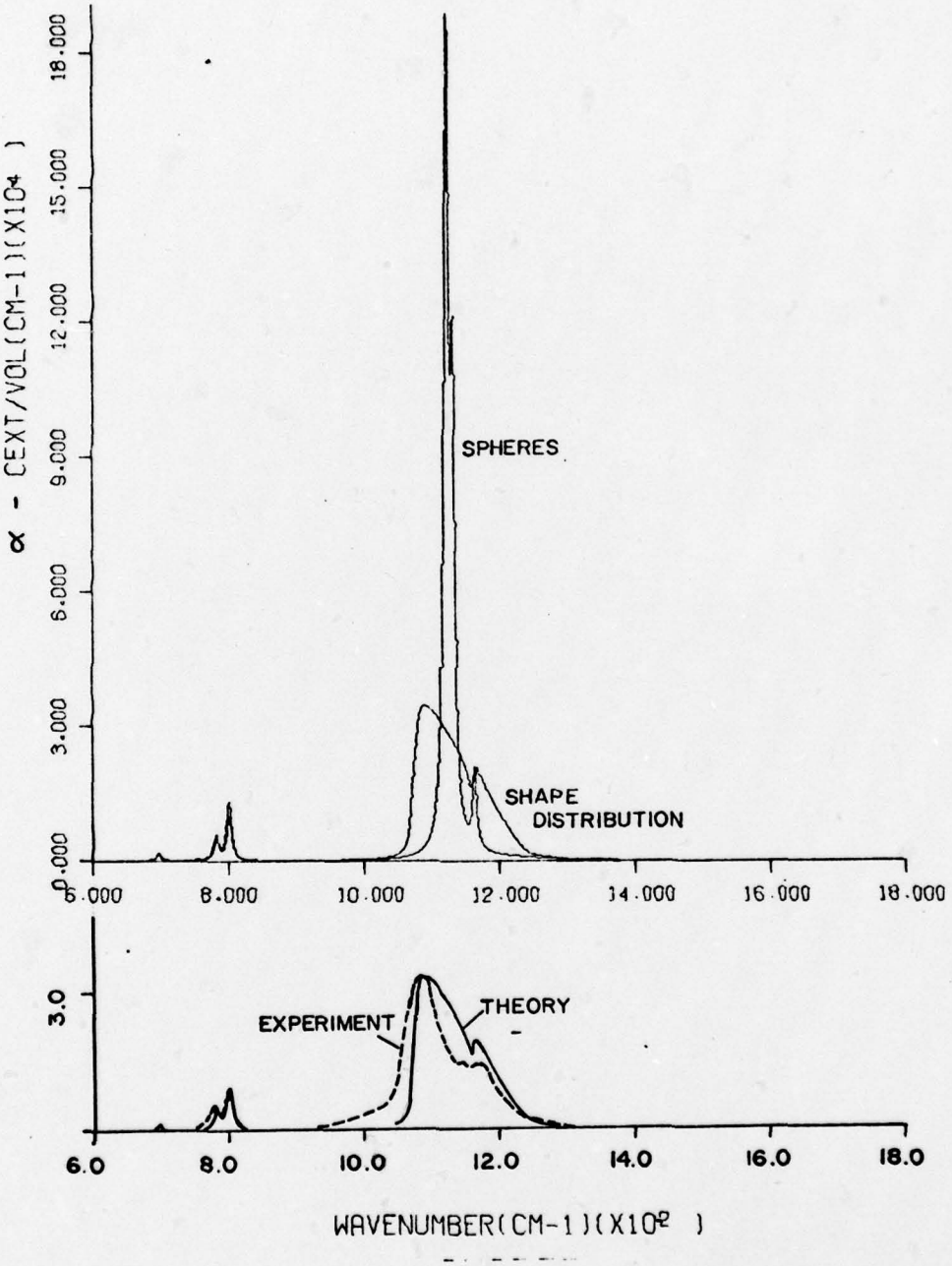

Figure 8: Comparison of calculated and measured extinction for quartz particles. The upper curves compare calculations for a continuous shape distribution of Rayleigh ellipsoids (CDE) with calculations for spheres. The lower curves compare the CDE calculations with measurements.

obvious that the accounting for of shape distribution has markedly improved the agreement of theory and experiment and shows promise of enabling us to extract optical constants for real powders composed of highly irregular particles.

IV. THEORY OF SHAPE DISTRIBUTION IN THE RAYLEIGH ELLIPSOID APPROXIMATION

The average absorption cross section for a collection of randomly oriented identical homogeneous ellipsoids that are sufficiently small compared to the wavelength of the incident light may be written in the form (van de Hulst 1957, chap. 6)

$$\langle C_{abs} \rangle = kv/3 \, \mathrm{Im} \left\{ \sum_{j=1}^{3} (\beta + L_j)^{-1} \right\} , \qquad (8)$$

$$\beta = (\epsilon - 1)^{-1} ,$$

where $v = 4\pi abc/3$ is the volume of an ellipsoid with semiaxes of length $a \geq b \geq c$; $\epsilon = \epsilon_1 + i\epsilon_2$ is the complex dielectric function of the particle relative to that of the surrounding medium, and $k = 2\pi/\lambda$ is the wave number of the surrounding medium. The L_j's are geometrical factors related to the ratios of semi-major axes for the ellipsoid (van de Hulst 1957, p. 71). Only two of the geometrical factors, which we shall take to be L_1 and L_2 are independent because of the relation

$$L_1 + L_2 + L_3 = 1 .$$

Suppose now that, in addition to being randomly oriented, the collection consists of all possible ellipsoidal shapes; i.e. the geometrical factors are not restricted to a single set of values but are distributed according to some shape probability function $\mathcal{P}(L_1, L_2)$. All ellipsoidal shapes are represented by points in the shaded triangular region shown

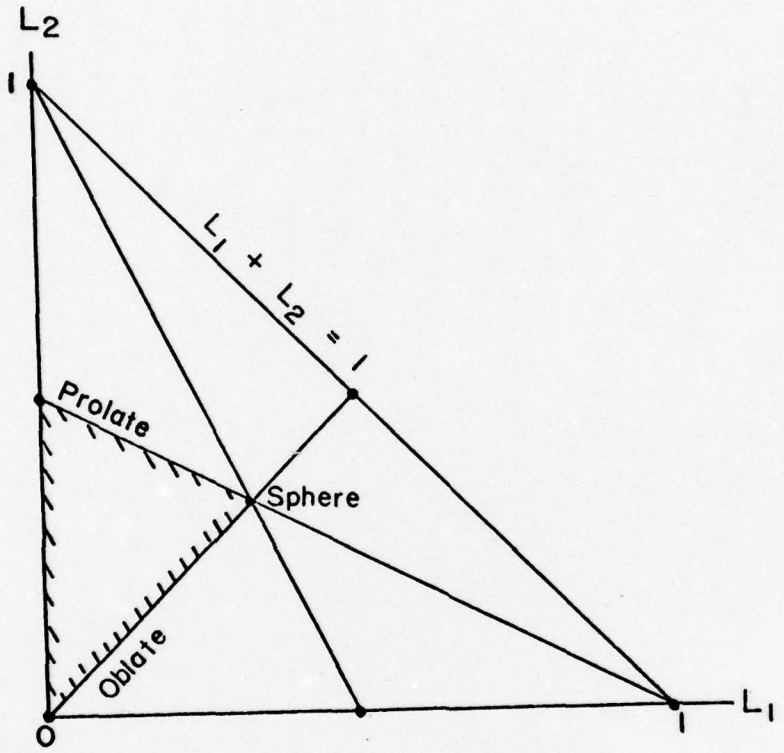

Figure 9: Domain of definition of the shape probability function. Outside of the region Γ bounded by $L_1 = 0$, $L_2 = 0$, $L_1 + L_2 = 1$, $\mathcal{P}(L_1, L_2)$ vanishes identically.

in figure (9). However, it is convenient for purposes of integration to define ρ on the larger triangular region Γ, which is composed of six equal area regions, each of which corresponds to one of the six possible ways of choosing the relative lengths of the ellipsoid axes a, b, c. The shape probability function is normalized to unity on Γ:

$$\iint_{\Gamma} \rho(L_1, L_2)\, dL_1\, dL_2 = 1 \qquad (9)$$

The absorption cross section averaged over the shape distribution and over all orientations is, therefore,

$$\langle\langle C_{abs} \rangle\rangle = \iint_{\Gamma} \langle C_{abs} \rangle \rho(L_1, L_2) dL_1\, dL_2 \qquad (10)$$

$$= kv/3\ \mathrm{Im}\ \{ \mathcal{I}_1 + \mathcal{I}_2 + \mathcal{I}_3 \},$$

where

$$\mathcal{I}_1 = \iint \frac{\rho(L_1, L_2)}{\beta + L_1}\, dL_1\, dL_2$$

$$\mathcal{I}_2 = \iint \frac{\rho(L_1, L_2)}{\beta + L_2}\, dL_1\, dL_2$$

$$\mathcal{I}_3 = \iint \frac{\rho(L_1, L_2)}{\beta + 1 - L_1 - L_2}\, dL_1\, dL_2$$

and $\beta = (\epsilon - 1)^{-1}$. The integral of a function $f(L_1, L_2)$ over Γ may be written as an iterated integral:

$$\iint_{\Gamma} f(L_1, L_2)\, dL_1\, dL_2 = \int_0^1 dL_1 \int_0^{1-L_1} f(L_1, L_2) dL_2$$

We have assumed that all particles have the same volume v; however, if there is no correlation between shape and volume, then the total absorption cross section of the collection is

$$\eta \frac{k\langle v\rangle}{3} \operatorname{Im}\{\mathcal{A}_1 + \mathcal{A}_2 + \mathcal{A}_3\}$$

where η is the total number of particles per unit volume and $\langle v\rangle$ is the average particle volume. It has also been implicitly assumed that $\rho(L_1,L_2)$ is continuous; this is not a necessary restriction, however, and we can take into account discrete distributions by replacing the above integrals with summations over the discrete set of points (L_1,L_2) in Γ.

Perhaps the simplest conceivable distribution is one for which all shapes are equally probable, in the sense that $\rho(L_1,L_2) = 2$, and the integrals are readily evaluated

$$\mathcal{A}_1 = \mathcal{A}_2 = \mathcal{A}_3 = \frac{2\varepsilon}{\varepsilon - 1} \log\varepsilon \quad -2 \quad .$$

Therefore, the average cross section is

$$\langle\langle C_{abs}\rangle\rangle = k\langle v\rangle \operatorname{Im}\left\{\frac{2\varepsilon}{\varepsilon-1} \log \varepsilon\right\} \quad . \qquad (11)$$

In the above expression log denotes the principal value of the logarithm of a complex number $z = re^{i\theta}$ (Churchill 1960, p. 56):

Other functions $\rho(L_1,L_2)$ could be chosen to represent a shape distribution of particles. The one chosen has the advantage of uniformity in the L_1L_2 plane of figure (9) and simplicity of the resulting expression (11). The real test of its practical value, of course, lies in how well it describes the properties of actual particles.

V. DIRECT COMPARISON OF EXPERIMENTAL AND THEORETICAL EXTINCTION MEASUREMENTS

Having developed a theoretical approach for treating nonspherical particles in the Rayleigh approximation and having successfully developed an experimental procedure for limiting the particle sizes to the small size range, we now seek to find how well the theory and experiments agree for several solids with already well known optical constants. In this section, then, we compare experimentally determined extinction spectra with calculated extinction spectra based on the known optical constants. This is the direct problem. The indirect problem, which is our ultimate interest, will treat the optical constants of these solids as unknown to see how well our inversion technique can determine optical constants. This will be the subject of section VI.

Four solids have been selected that have strong absorption bands in the 8 to 20 μm spectral range. The main criterion for selection of these "standard" solids is that their bulk optical constants be already well known from conventional measurements on single crystals. The solids chosen are quartz (SiO_2), calcite ($CaCO_3$), SiC, and NiO. All of these solids were available commercially as fine powder. NiO is the only truly isotropic solid and was chosen partly for that reason. SiC is iniaxial but only slightly so. It is of interest because it has one of the largest calculated extinction peaks near 10 μm of any solid we have found. Quartz and calcite are both very common minerals that are anisotropic. Calcite is particularly anisotropic and was chosen primarily for this reason.

A. Sample preparation and measurements

Samples of small sized powders dispersed in KBr pellets were prepared for extinction measurements in the following way:

(1) The solid was either acquired as a fine powder or

bulk material was ground in a ball mill to produce a fine powder. Most solids are available from the manufacturer as a fine powder since many of the production techniques, such as wet chemical precipitation, give rise to such a form. All the materials reported on in this study were in fact purchased as powdered material.

(2) The powder was segregated by Stokes' law settling in either water or alcohol. Some details of this have already been given in section III. After dispersal of the powder in the liquid the dispersion was allowed to stand overnight, after which the top portion of the liquid was drawn off and dried in a glass dish on a hot plate for a sufficient number of hours to drive off the water.

(3) A small quantity of the sample powder (of the order of .5 milligram) was weighed and mixed with about 0.5 gm of KBr powder by agitation of the mixture in a small glass vial with steel balls for 12 hours or more. This appears to be necessary in order to break up clumps of powder and to insure uniform dispersal.

(4) A 1/2" diameter pellet of KBr and sample was pressed from the powder mixture in a special pellet die obtained from Barnes Engineering Company. Ten tons of force were used, resulting in pellets that are almost transparent in visible light. Transmission spectra (T vs. wavelength) were recorded with a Perkin Elmer model 137 spectrophotometer with a pure KBr pellet in the reference beam to correct for reflection at the KBr surfaces.

(5) Volume extinction coefficients (α) were calculated from the expression

$$T = \exp\left(-\alpha\frac{\sigma}{\rho}\right)$$

where σ is the mass density of sample per unit cross sectional area determined from the weight of the powder and the dimension of the pellet. The bulk density of the solid is denoted by ρ.

B. Extinction results compared with theory

Figures (10-13) show the comparison of measured extinction coefficients with calculations for spheres and for a distribution of Rayleigh ellipsoids using equation (11). Optical constants derived from bulk solid measurements reported in the literature were used in the calculations. References to the published optical constants are given in table II.

Table II

Sources of the measured optical constants used

Solid	Reference
quartz (SiO_2)	Spitzer and Kleinman (1961)
calcite ($CaCO_3$)	Hellwege et. al. (1970)
α-SiC	Spitzer, Kleinman and Walsh (1959)
NiO	Gielisse et. al. (1965)

Generally, the distribution of ellipsoid calculations (CDE) come much closer to matching the measurements in magnitude and shape of the extinction feature than do the sphere calculations. In the case of quartz the agreement in magnitude, width and shape of the bands is excellant. For $CaCO_3$ there is about a factor of two discrepancy remaining between the CDE and measurements, but the improvement over the spherical theory is substantial. The magnitude agreement between CDE and measurements is good for SiC although measurements show a rather extended tail of absorption to lower frequencies. It is possible that this tail is due to the presence of other forms of SiC in the powder than the α-SiC for which theoretical calculations were made. SiC occurs in a number of different crystalline forms (see the various articles in O'Conner and

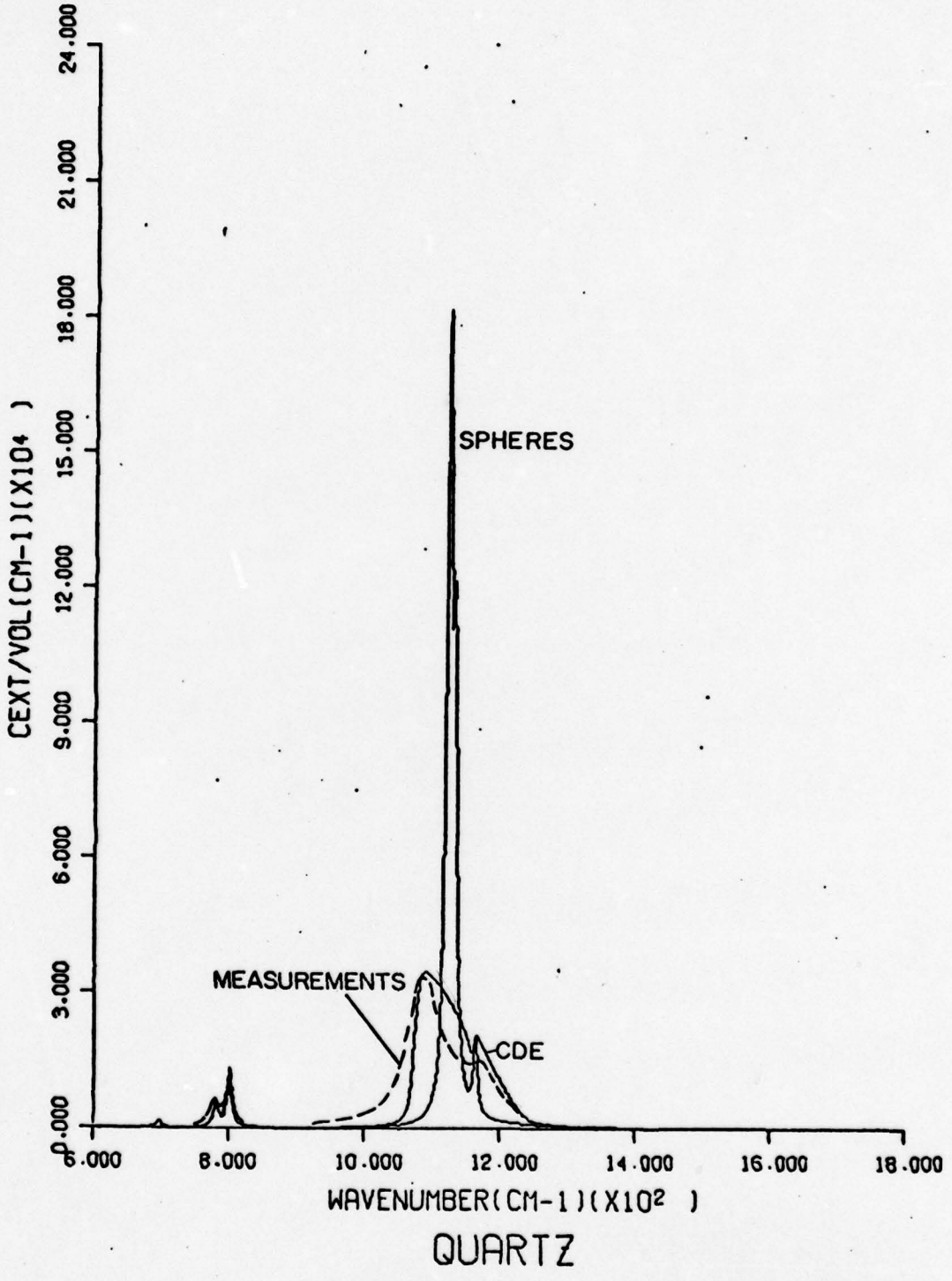

Figure 10: Comparison of measured extinction (dashed curve) for quartz powder in KBr with calculations for spheres and for a distribution of ellipsoidal shapes (CDE) in th Rayleigh approximation.

Figure 11: Comparison of measured extinction (dashed curve) for calcium carbonate powder in KBr with calculations for spheres and for a distribution of ellipsoidal shapes (CDE) in the Rayleigh approximation.

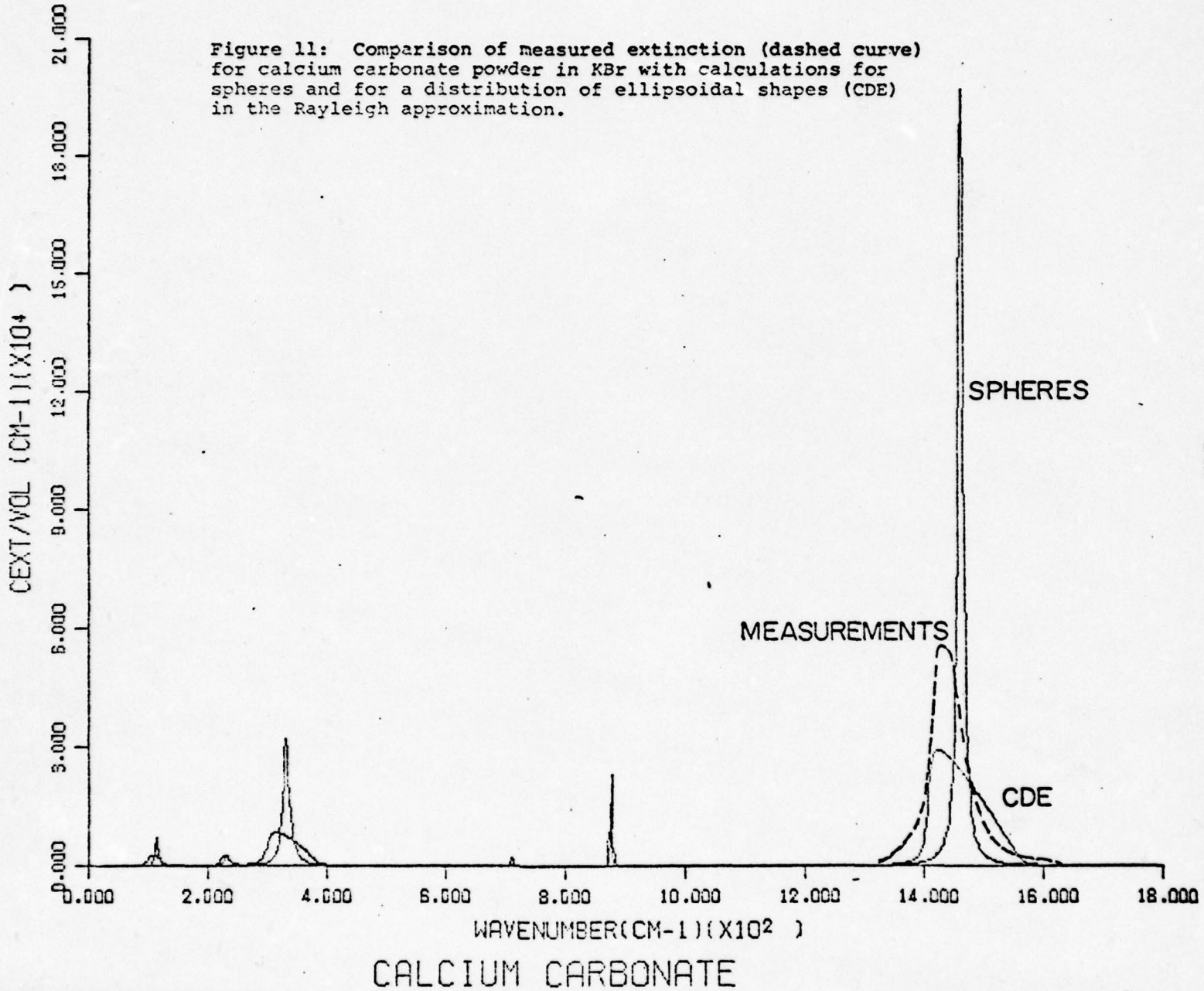

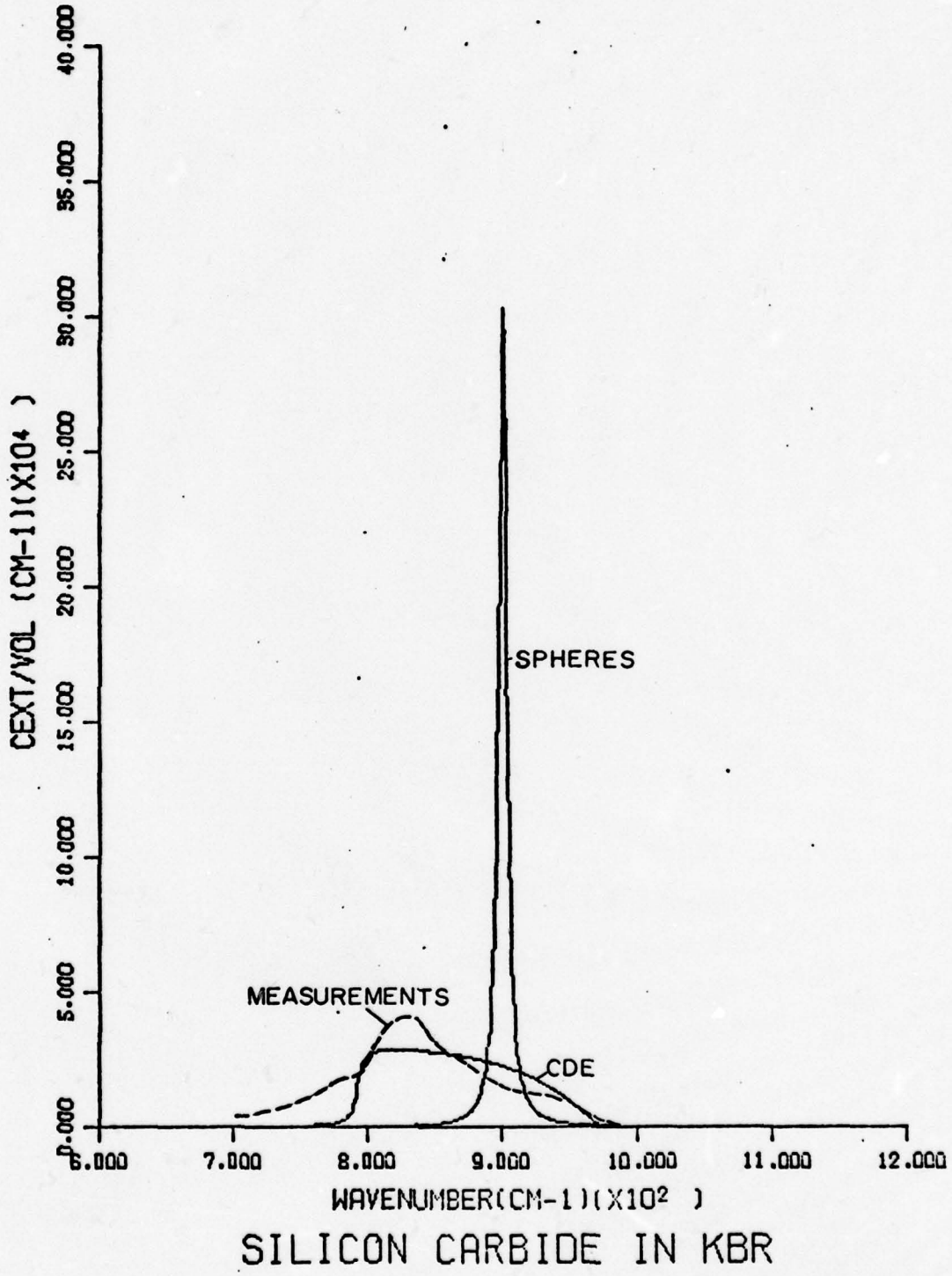

Figure 12: Comparison of measured extinction (dashed curve) for SiC powder in KBr with calculations for spheres and for a distribution of ellipsoidal shapes (CDE) in the Rayleigh approximation.

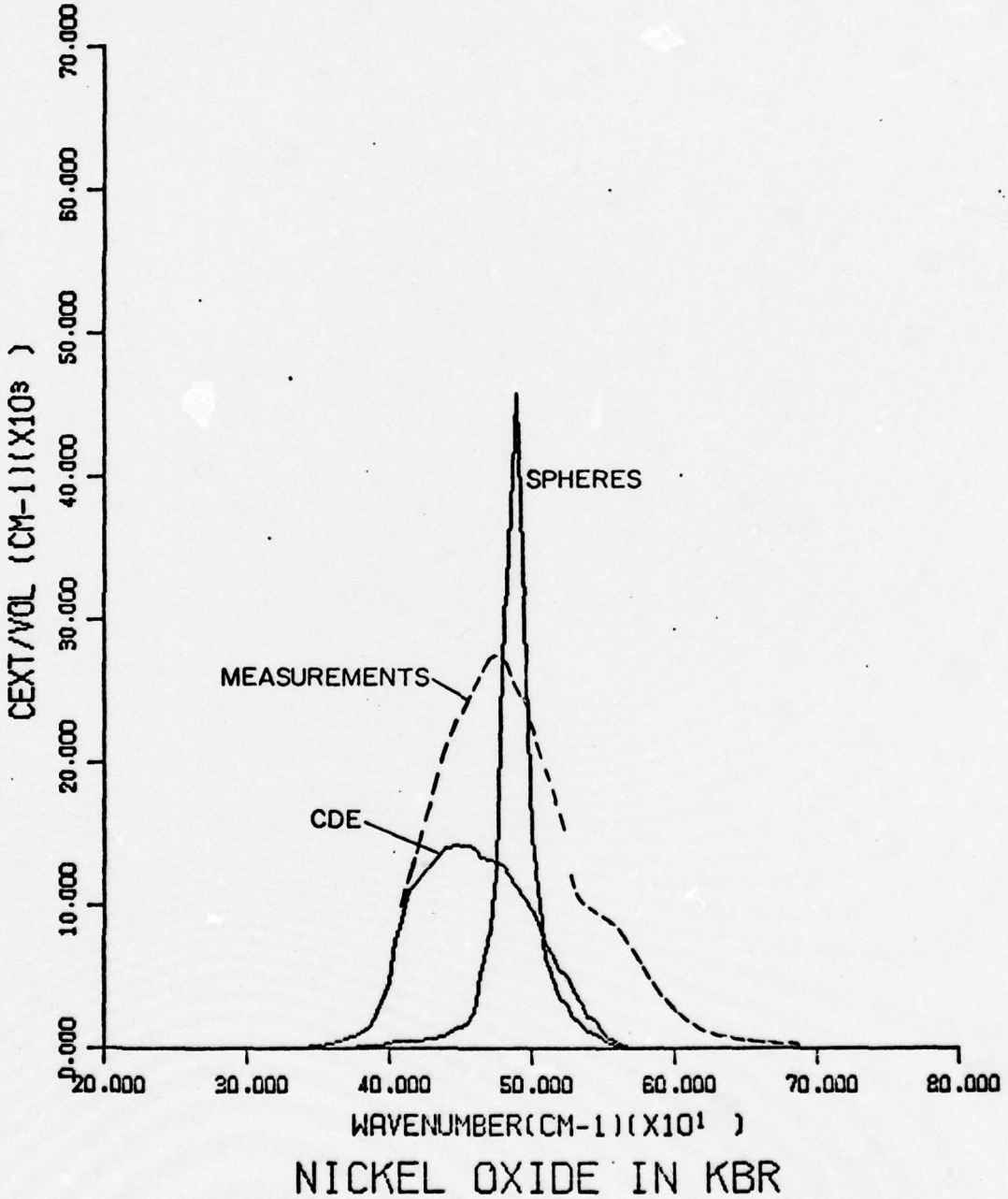

Figure 13: Comparison of measured extinction (dashed curve) for NiO powder in KBr with calculations for spheres and for a distribution of ellipsoidal shapes (CDE) in the Rayleigh approximation.

Smiltens 1959). Our information supplied by the manufacturer gave no idea of the percentage of SiC polytypes present in the powder. In the case of NiO the maximum of the measured extinction falls about half way between the sphere calculations and the ellipsoid distribution calculations, but the shape and width of the extinction is modeled more correctly by the CDE. The fact that the peak extinction measurements are higher than the CDE curves in the cases of calcite and NiO probably implies that the particles are a little closer to being spheres than to the wide shape distribution described by our distribution function of equation (9). Indeed it is reasonable that this shape distribution might be too "drastic". A numerical integration over L values more closely surrounding the sphere point ($L_1=L_2=1/3$) in figure (9) might be better. Further work along these lines is planned in the next year's work. Because of the integrability of the shape distribution function $\wp(L_1, L_2) = 1$ and because it does seem to give a rather good representation of extinction for some solids, we continue to use it for our attempted inversions of the data.

VI. INVERSION OF THE EXTINCTION DATA TO OBTAIN OPTICAL CONSTANTS

The preceeding results have shown that the new treatment of particle shape distribution gives substantially better agreement with extinction measurements on real particles than does sphere theory, even though the new theory is not entirely satisfactory in every case. We now use the measured extinction spectra for our model solids (the dashed curves of figures 10-13) as input for calculations to determine optical constants. In this way we treat the optical constants as unknown for these solids and evaluate our determinative procedures to see how accurately the derived optical constants agree with the known optical constants for these materials.

A. The method

The process uses an interactive computer with which the operator can repeatedly adjust the input parameters into theoretical calculations of extinction until the calculated spectrum converges satisfactorily close to the measured spectrum. The computer is programmed with the theoretical equations, which are combinations of the Lorentz oscillator theory for ε(4) followed by the extinction theory for a shape distirbution of Rayleigh ellipsoids. The principal equations are the Lorentz multiple oscillator equation for complex ε

$$\varepsilon = \varepsilon_\infty + \sum_j \frac{\omega_{p,j}^2}{\omega_j^2 - \omega^2 + i\gamma_j\omega} \qquad (4)$$

and the shape distribution equation (CDE)

$$\langle\langle C_{abs} \rangle\rangle = k\langle v \rangle \, \mathrm{Im}\left\{ \frac{2\varepsilon}{\varepsilon - 1} \log \varepsilon \right\} . \qquad (11)$$

Input parameters are the oscillator parameters

$$\varepsilon_\infty, \ \omega_j, \ \omega_{p,j}, \text{ and } \gamma_j \quad .$$

Although it might at first seem to be a hopeless task to vary so many parameters, a little experience with the Lorentz theory enables one to make excellant estimates of some of the parameters in the beginning, as we now indicate. First, the ε_∞ can often be found from handbook or literature values since for most insulating solids it is equal to the square of the index of refraction in the visible or near infrared. This quantity can be determined, even on microscopic particles of a solid, by varying an immersion oil's index of refraction until the particle as viewed under the microscope appears to vanish. The

oil and the particle then have identical indices of refraction. A discussion of this technique along with an extensive collection of n values is found in The Particle Atlas (McCrone and Delly 1973).

Next one must determine the number of oscillators, j, by considering the number of resolvable peaks in the extinction curve for the frequency range of interest. In most cases of strong infrared extinction there will be only one dominant oscillator near the region of interest. This is true of $CaCO_3$ as regards the 1500 cm^{-1} region, for example. In NiO, one major oscillator giving an extinction peak near 480 cm^{-1} is suggested, although further weaker extinction appears to be present near 580 cm^{-1}. In the case of quartz there appear to be two main, overlapping extinction bands, near about 1090 and 1150 cm^{-1}. These examples show that the first estimate of j is not difficult. Estimation of ω_j and ω_p is greatly aided by a little familiarity with the behaviour of the oscillator equations. Shape broadened extinction bands for the extremely intense bands of concern in this work are well confined to the frequency region for which ε_1 is negative (see paragraph 4.3 of the review article by Huffman 1977). The low frequency limit of this negative ε_1 region coincides closely with ω_j for an isolated band. This enables one to make a good estimate of ω_j immediately. The high frequency limit of the extinction band occurs at the point where $\varepsilon_1 = 0$. Since absorption is low in this region one can reasonably neglect the damping term in the denominator of equation (4) and set $\varepsilon_1 = 0$. These approximations are indicated below.

$$\varepsilon = \varepsilon_1 = 0 = \varepsilon_\infty + \frac{\omega_p^2}{\omega_0^2 - \omega^2 + i\gamma\omega} \quad (\gamma\omega \to 0) = 0$$

Solving for ω and calling it $\omega(\varepsilon=0)$

$$\omega(\varepsilon=0) = \left[\frac{1}{\varepsilon_\infty} \omega_p^2 + \omega_0^2 \right]^{1/2} \qquad (12)$$

The only oscillator parameters left to be chosen are the damping factors γ. Usually, for strong bands $\gamma\omega << \omega_0^2$ which puts some limits on γ. Beyond this it is probably best to determine by making a few trials at matching the measured extinction on the computer. Following these first guesses, any of the oscillator parameters may need to be corrected and other less important oscillators added.

A brief summary of the techniques suggested for making the first guesses is as follows:

(1) Select ε_∞ from handbook or literature values.

(2) Select ω_0 from the low frequency edge of the extinction band.

(3) Estimate ω_p from the high frequency edge of the extinction band using equation(12).

(4) Determine the remaining parameter γ by computer iteration to match the data.

Lest the reader feel that this is a terribly subjective and "hit or miss" technique, we want to point out that this is exactly analogous to the time-tested oscillator method for determining optical constants of bulk solids from normal incidence reflectance data. Most of the single crystal optical constants referenced in table II have been derived in such a way. The only difference is that, in the present case, the theory incorporates the much more complicated extinction for a distribution of shapes rather than the simple and unquestionably applicable Fresnel equation (2) used in the bulk studies.

Treatment of Anisotropy

The above technique has assumed that the solid is isotropic, i.e. that its optical constants are the same for all polarization directions. A crystalline solid, however, may be either isotropic (all directions the same), uniaxial (two major polarization directions), or bi-axial (three major polarization directions). The difference these cases would make in the extinction expression (11) is indicated below:

$$\langle\langle C_{abs} \rangle\rangle / k\langle v \rangle = \text{Im}\{\} \quad \text{isotropic solids}$$

$$= 2/3\ \text{Im}\{\} \quad \text{uniaxial with } E \perp c$$

$$= 1/3\ \text{Im}\{\} \quad \text{uniaxial with } E \parallel c \text{ or bi-axial}$$

$E \perp c$ and $E \parallel c$ denote the electric field orientation perpendicular and parallel respectively to the unique axis c. For purposes of inversion we have merely assumed that the optical constants are isotropic. This could result in an error as large as a factor of three in the absorption attributed to a given band. One could rather assume the factor 2/3 so that the maximum error in absorption would be a factor of 2. It should be pointed out that this magnitude of error does not necessarily propagate into the optical constants. Further work should be done, however, on the problem of how to select the factor.

B. Results of the inversion procedure

Results of the scheme for obtaining optical constants are presented in figures (14) through (17). Derived dielectric functions are shown as dashed lines and the "true" (measured for single crystals) dielectric functions are represented by full lines. The scales of the figures have been chosen to emphasize the regions of most consequence in determining small

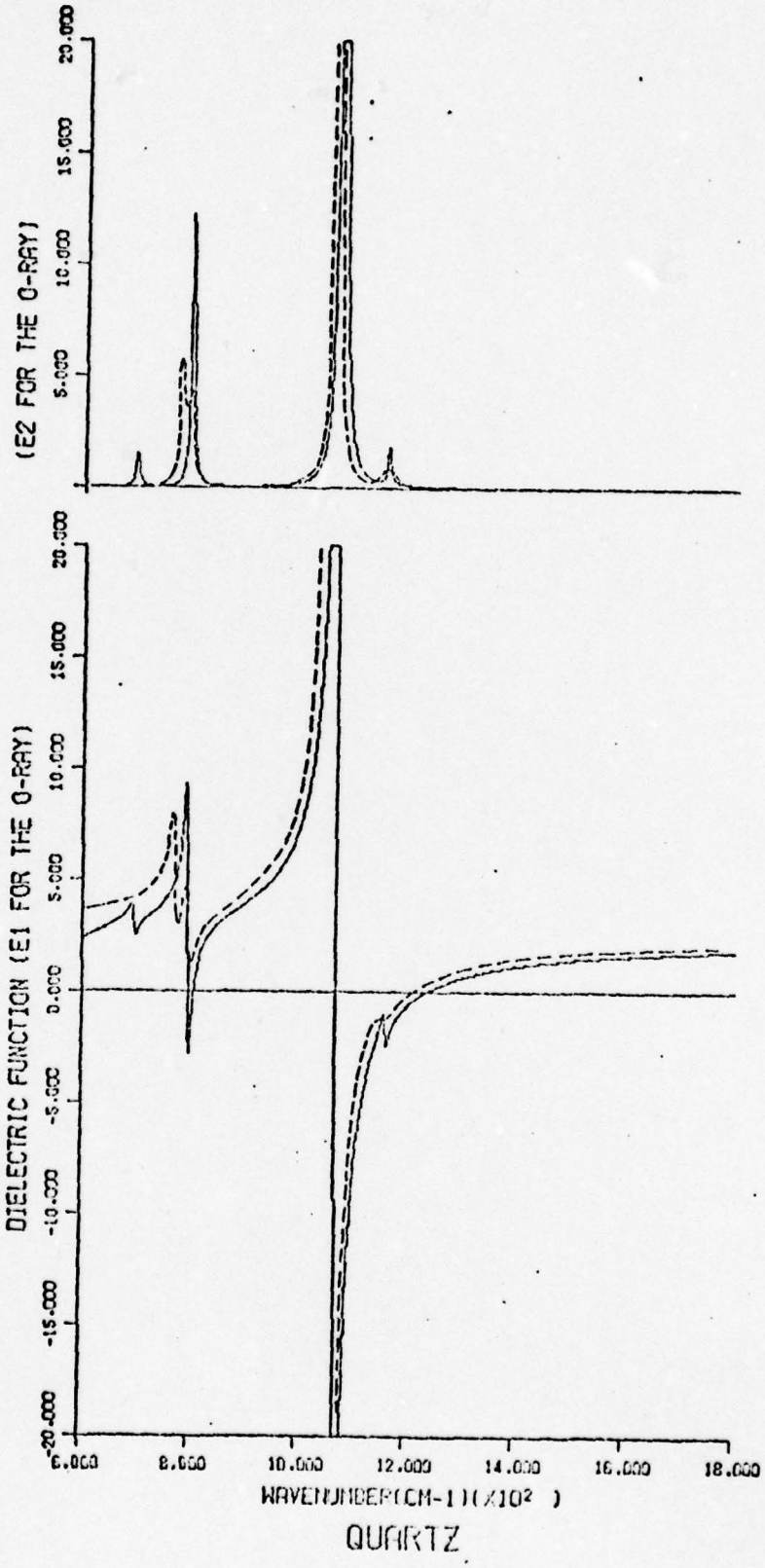

Figure 14: Results for quartz of the inversion of powder extinction data to infer dielectric functions (dashed curve) compared with dielectric functions derived from single crystal measurements (solid curve from the reference in Table II). Only one set of curves (the O-ray) of the uniaxial crystal quartz are shown for clarity. Both directions have similar optical constants in the most prominent band near 1100 cm^{-1}.

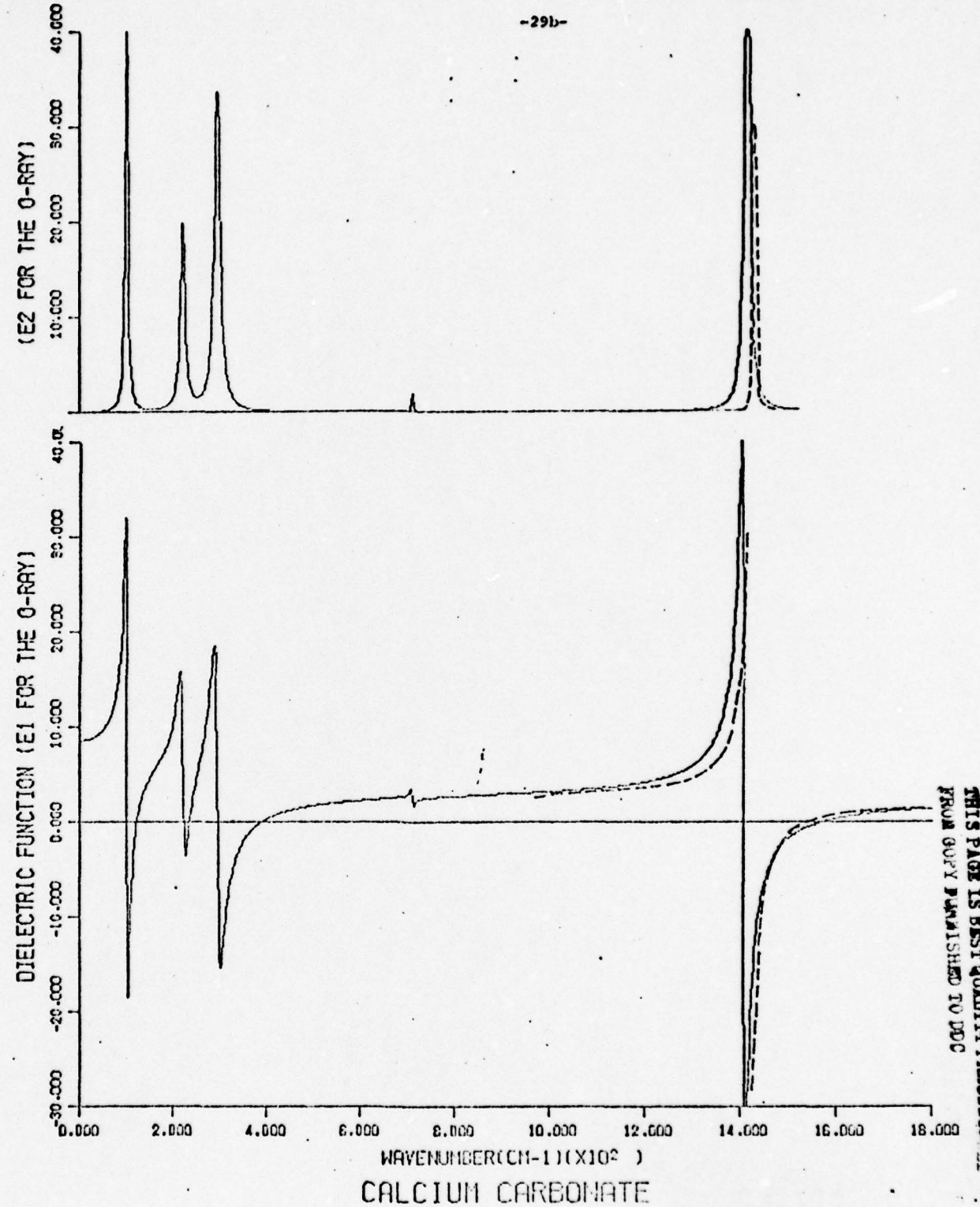

Figure 15: Results for calcium carbonateof the inversion of powder extinction data to infer dielectric functions (dashed curve) compared with dielectric functions derived from single crystal measurements (solid curve from the reference in Table II).

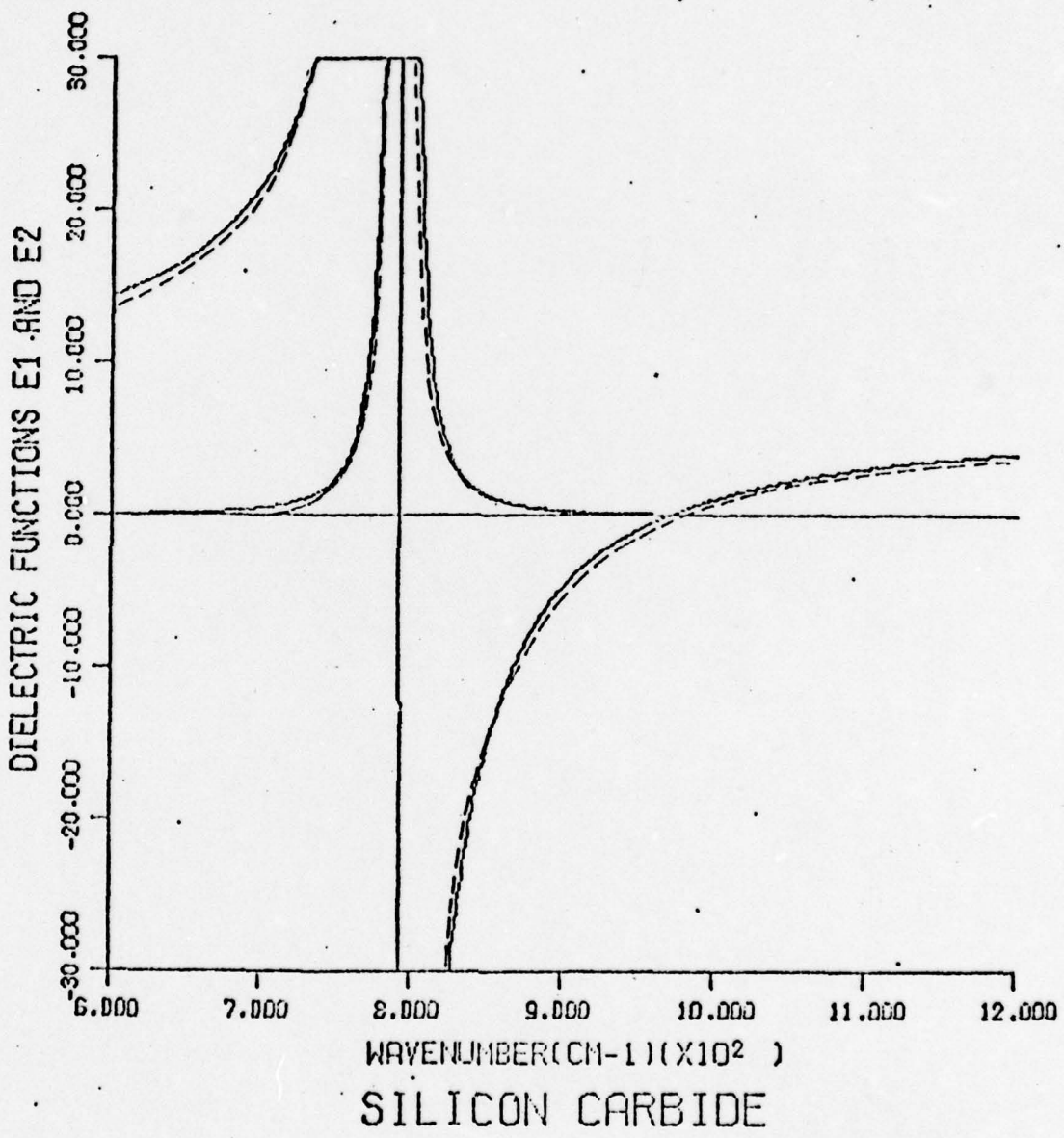

Figure 16: Results for silicon carbide of the inversion of powder extinction data to infer dielectric functions (dashed curve) compared with dielectric functions derived from single crystal measurements (solid curve from the reference in Table II).

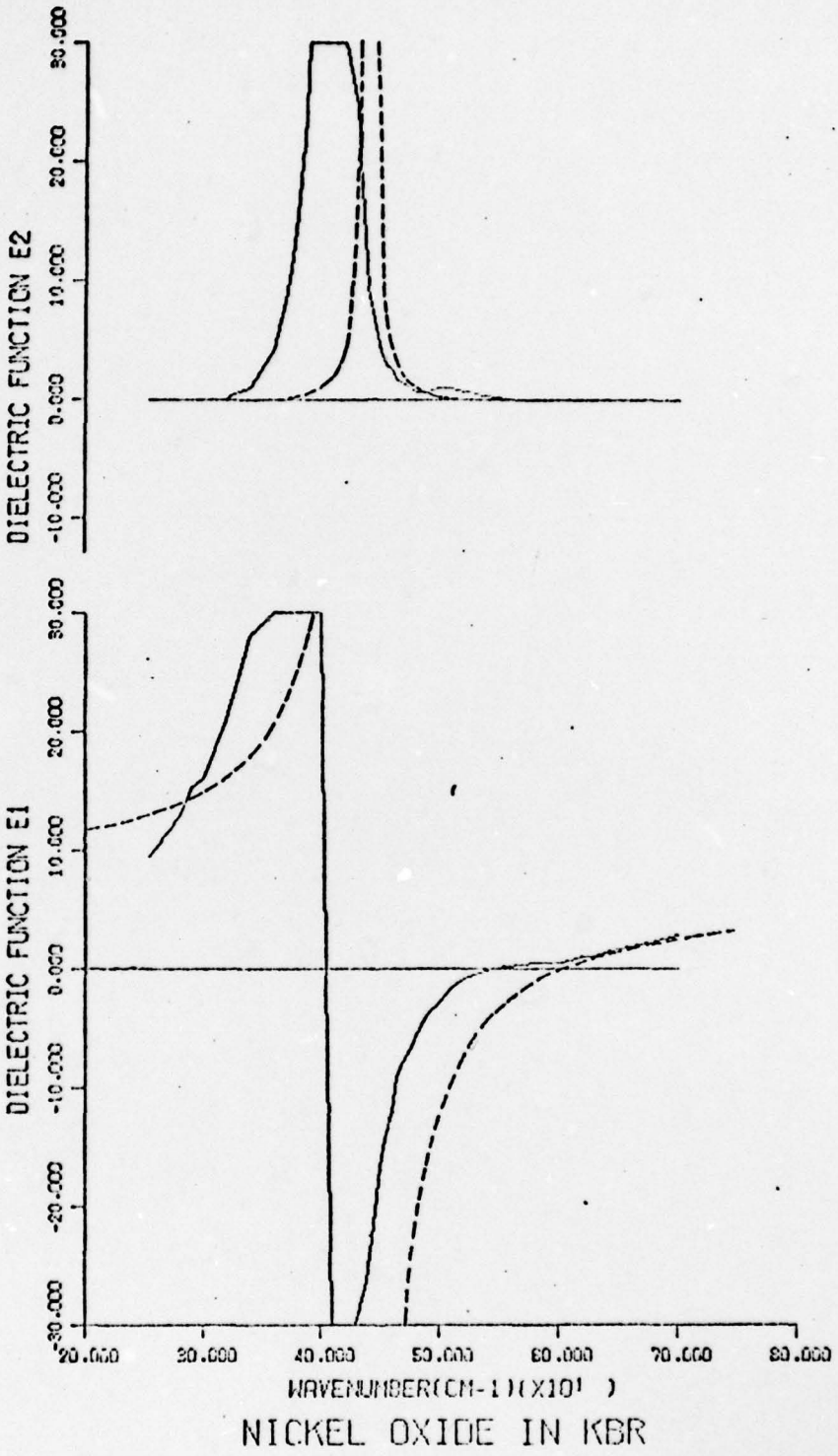

Figure 17: Results for NiO of the inversion of powder extinction data to infer dielectric functions (dashed curve) compared with dielectric functions derived from single crystal measurements (solid curve from the reference in Table II).

particle extinction properties, although this emphasis truncates the extreme excursions of ε_1 and ε_2. In the case of quartz the powder results compare very well with measured bulk constants. Crystalline quartz has two sets of optical constants, one set for the ordinary (O) ray and one set for the extraordinary (E) ray. For the large feature near 1050 cm^{-1} the measured optical constants are very similar for the two directions and only one set is shown to minimize confusion in figure (14). Since the optical constants in the two directions are so similar near 1050 cm^{-1} the crystal acts very much like an isotropic crystal, which our fitting procedure has assumed. For the structure near 800 cm^{-1} there is more difference for the two directions, and the powder results contain structure from each polarization direction. The silicon carbide results are very close to bulk measured properties -- so close that the agreement may contain an element of good luck. However, the true optical constants for SiC are acurately modeled very well by a one oscillator fit with very low γ. Since our procedure has little sensitivity to small γ's, only the two parameters ω_0 and ω_p need be chosen correctly; these have evidently been chosen quite well in the fitting procedure. The NiO results, figure (17), are not so favorable in comparison with measured values. In the case of $CaCO_3$ the results are rather good despite the fact that the anisotropy is not taken into account in the inversion. We treated the situation as though it was an unknown for which we had no knowledge of whether the band near 1400 cm^{-1} is present in one, two or three of the major polarization directions. The bulk optical constants in the comparison are for the O-ray which is totally responsible to the band. Overall, the inversion technique for determining optical constants of powders gives results which compare quite favorably with measured bulk values for the cases of our four comparison solids.

VII. COMMENTS ON THE SEARCH FOR MAXIMUM EXTINCTION

Although our primary goal has been the development of a technique for determining optical constants, the process of repeatedly going back and forth between calculations and experiment for a number of solids has provided some insights into the larger problem of how to produce maximum extinction in the infrared. Several points of this nature which were not fully realized by us at the beginning of this work will now be discussed briefly.

A. Selection of the resonant frequency

The equation (8) for extinction by a Rayleigh ellipsoid clearly shows that a resonance of the sort we have been concerned with can be made to occur at any point in the negative ε_1 region by varying the relative dimensions of the ellipsoid to change the L_j. The resonant condition follows directly from minimizing the denominators of each term of equation (8), giving rise to

$$\varepsilon_1 = -\varepsilon_m[1/L_j - 1] \qquad (13)$$

This equation is also discussed in some detail by Huffman (1977). To exemplify the placement of the ellipsoid resonances we have calculated extinction for a randomly oriented ellipsoid of SiC with the particular L_j's of .1, .3, and .6. The results are shown in figure (18) along with our CDE calculations and the real part of the dielectric function which determines the ellipsoid resonance position according to the above formula. In this crystal the range of possible resonance frequencies is from about 780 cm^{-1} to about 960 cm^{-1}. One notices that the spread of the shape distribution calculation is between these

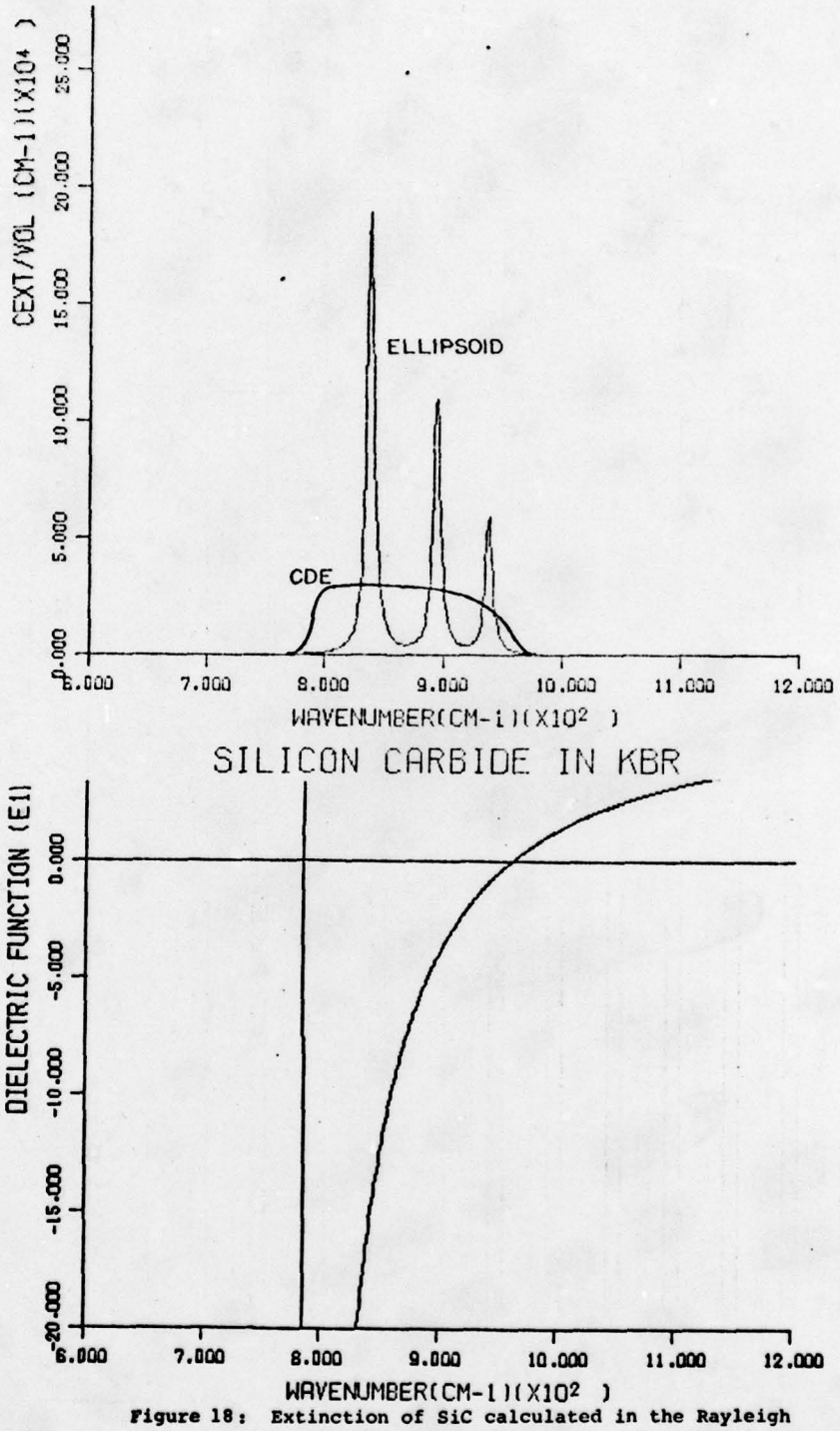

Figure 18: Extinction of SiC calculated in the Rayleigh ellipsoid approximation for randomly oriented identical ellipsoids with shape parameters L_j = .1, .3, and .6, and for a continuous distribution of ellipsoidal shapes (CDE). The real part of the complex dielectric function, which determines the positions of the peaks, is shown below.

limits and the three ellipsoid peaks fall in the same region.

In the case of metallic solids it is possible to choose the resonance frequencies over a much wider range. The negative ε_1 region for many metals ranges from the plasma frequency, which is characteristically in the far ultraviolet, through the visible, infrared, and microwave regions to zero frequency. Thus a resonance in a metal particle could conceivably be designed to occur at any frequency in the infrared. A calculated example of extinction for one particular ellipsoid (L_j= .01, .3, and .69) of aluminum is shown in figure (19). Once again the CDE calculation and the ε_1 curve are given for comparison. These two illustrations emphasize the important point that the resonance positionsof a single ellipsoidal shape can be selected if one can control the shape parameters; however, a distribution of shapes inevitably decreases the strength of the extinction while giving a broader extinction band. It appears to be technologically impossible to produce a cloud of sub-micron particles composed of identical ellipsoids, all having exactly the same, chosen axial ratios; therefore, it is perhaps more important to consider the extreme ellipsoidal shapes of spheres (L_j's = 1/3), discs (L_j= 1/2,1/2,0) and needles (L_j= 1,0,0). These shapes can frequently be taken by real particles.

B. Practical maximum extinction for spheres, needles, and discs

Since the heights and widths of the extinction peaks are determined by optical constants of the various solids, not many of which are known, it is not possible for one to say what the maximum possible extinction may be among all solids. We can, however, choose a few examples from promising ionic crystals having measured optical constants in the vicinity of their intense absorption bands in the infrared. Calculations for peak extinction normalized per unit volume of spheres, needles,

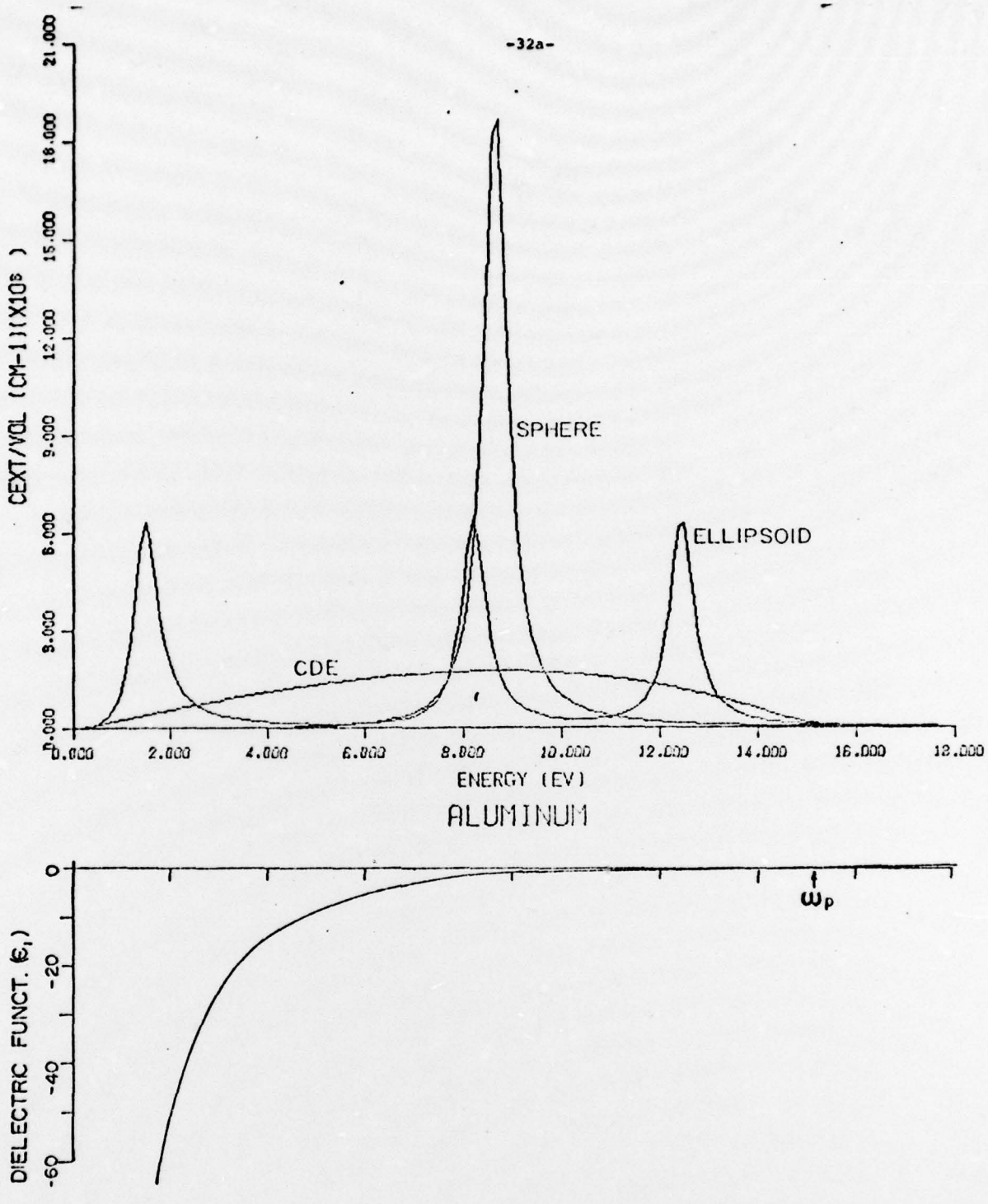

Figure 19 : Extinction of aluminum calculated in the Rayleigh ellipsoid approximation for randomly oriented identical ellipsoids with shape parameters L_j = .01, .3, .69 and for a continuous distribution of ellipsoidal shapes (CDE). The real part of the complex dielectric function, which determines the positions of the peaks, is shown below.

and discs of three solids are listed in Table III. The metal aluminum is included in the three for comparison.

The first important point to observe is that the sphere wins in all cases in the competition for maximum extinction among the three limiting shapes in the vicinity of their shape-dependent resonances. The magnitude of the maximum extinction for spheres is determined by how small ε_2 is at the resonance frequency. For these examples the maximum value of extinction is about 4×10^5 cm^{-1} in the vicinity of 10 μm. For the present, at least, this represents about the maximum expected extinction per unit volume for spheres of real material.

C. Practical maximum extinction for shape distributions

It has already been discussed that a distribution of shapes gives a broader but less intense extinction band than single shapes. If the CDE expression is applicable to real particulates one can determine an approximate upper limit for extinction by a collection of irregular particles, since equation (11) usually tends to a limiting value in the vicinity of the shape-dependent resonances with low damping. The reasoning follows:

$$\varepsilon/\varepsilon\text{-}1 \text{ is approximately } = 1$$

$$\text{Im}\{\log \varepsilon\} = \theta = \arctan \varepsilon_2/\varepsilon_1 \tilde{=} \pi$$

$$\therefore \quad \frac{\langle\langle C_{abs} \rangle\rangle}{v} \cong k\pi \cong (2\pi)^2/\lambda \quad .$$

For particles in air the limit is about 3×10^4 cm^{-1} for a frequency corresponding to about 10 μm wavelength. This limiting curve is shown in the last figure. Our highest extinctions measured in this work are consistent with this

Table III

Average Absorption Cross Sections per Unit Particle Volume for Randomly Oriented Rayleigh Spheres, Needles, and Discs at the Dipole Resonances for Each Shape

		MgO			SiC			Al		
	ε'	ε''	λ (μm)	$\langle C_{abs} \rangle / v$ (10^4 cm^{-1})	ε''	λ (μm)	$\langle C_{abs} \rangle / v$ (10^4 cm^{-1})	ε''	λ (μm)	$\langle C_{abs} \rangle / v$ (10^4 cm^{-1})
Sphere	-2	0.33	16.5	10.4	0.16	10.7	33.0	0.215	0.083	18.5
Needle	-1	0.32	15.3	3.4	0.11	10.5	14.5	0.13	0.116	11.1
Disc	0	0.10	13.7	1.6	0.085	10.3	2.3	0.05	0.143	5.1

limit or slightly greater. This might be considered to be the maximum extinction for a wide distribution of shapes.

The considerably larger peak extinction value of $\alpha = 2.1 \times 10^5$ cm^{-1} has been reported for a small size fraction of powdered talc (Dorschner et.al.1979), a mineral with the chemical composition $Mg_2(OH)_2(Si_2O_5)_2$ which is the primary basis for the common talcum powder. These measurements were discussed briefly by Bohren and Huffman (1979b) and are included in figure (20). It appears that the exceptionally large extinction values may be due to the particles being nearly spherical. Since talc is one of the softest of all solids, our speculation has been that in the process of forming the talc into a KBr pellet the high pressure molds the talc grains into an approximately spherical shape, considerably enhancing the peak extinction. An attempt was made to use our technique to invert the extinction data for talc using the ellipsoid distribution theory, but it was impossible to decrease γ enough to give calculated values as high as the measurements. In this special case, because of the softness of talc, it proved possible to press a pellet of pure talc with almost bulk density for specular reflectance studies. Analysis of the specular reflectance curve, treating the sample in this case as a smooth, bulk sample gave optical constants for extinction calculations. The results were that the CDE calculations peaked at about 2×10^4 cm^{-1} using the inferred optical constants, while the sphere calculations could be made to peak at about the measured valueof 2.1×10^5 by choosing a value of the damping constant within the uncertainty of the optical constants fit. The conclusion from this approach agrees with our earlier conclusion; that is that talc particles are much more spherical after being pressed into the pellet than most collections of particles in KBr.

C. Comparison of some extremes in infrared extinction

Our last figure (20) can be taken as a sort of summary of several things we have learned in relation to the search for maximum extinction in the 10 μm spectral region. A number of materials and limits are presented, all plotted in the same volume-normalized extinction units with no adjusted scaling. A phosphorous smoke aerosol, which is a common military screening smoke, has been plotted from the published measurements of Carlon et. al. (1977). Calculations on SiC for spheres and for a continuous distribution of ellipsoid shapes, which have been shown on a different scale in figure (12), represent extinction to be expected for spheres and for a wide distribution of shapes. Recall that measured extinction for SiC particles falls near the CDE calculations although the band shape is somewhat different. Talc measurements are included to indicate how large the extinction peak may be in some almost-spherical silicates. The practical maxima for spheres are shown as a series of dashed peaks to remind the reader that this level of extinction is appropriate only for narrow band absorption at a few, but not all, of the indicated wavelengths. Placement of the practical maxima for spheres is based entirely on a few solids for which we know ε_2 at the resonance position, and for talc. Also shown in figure (20) is the theoretical maximum for a distribution of shapes based on the saturation of our expression for a continuous distribution of Rayleigh ellipsoid shapes. A curve of the "practical upper limits" for absorption only, deduced by Carlon (1979), is included. It does not include effects which arise from strong variations of optical constants in the vicinity of an absorption, which has been the main emphasis of our work.

This collage of extinction information is meant to give an overview of representative maximum values that might occur in the 10 μm spectral region. Although the total picture may

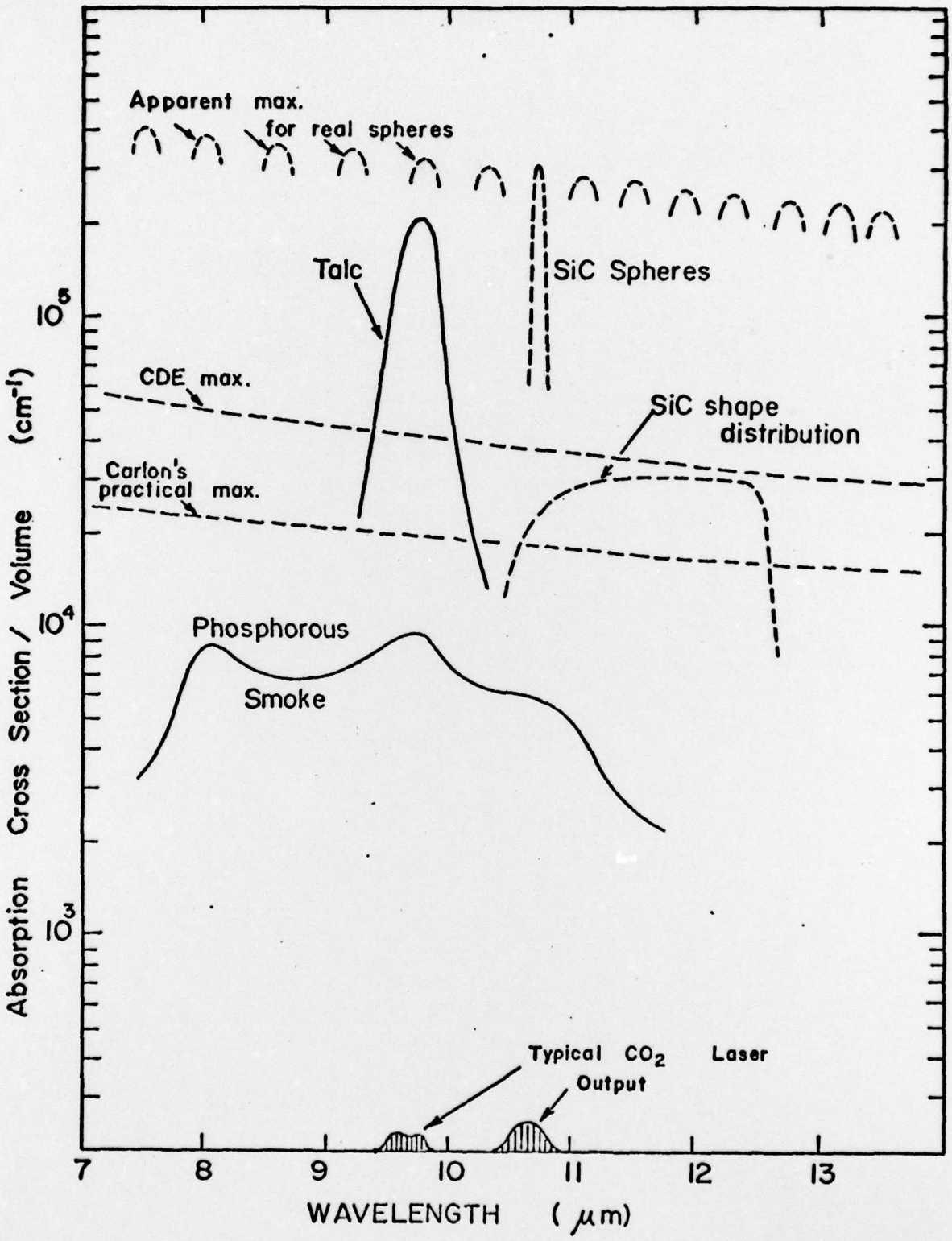

Figure 20: Volume-normalized extinction for a collection of several highly absorbing materials and for several practical limits discussed in the text.

still be a bit confused, one fact is clear. Spheres of certain materials having strong vibrational absorption bands in this region produce very intense, but quite narrow, extinction bands. To produce broader bands it appears to be necessary to reduce the maximum extinction, either by varying the shape distribution or by using solids with different optical constants.

VIII. CONCLUSIONS AND RECOMMENDATIONS FOR FUTURE WORK

The best method we have developed for deducing optical constants of powdered materials is to segregate a sub-micron size fraction, embed a weighed portion of the powder in a KBr pellet for transmission measurements, and fit the measured results with a theory composed of Lorentz oscillator expressions and Rayleigh theory for extinction by a distribution of ellipsoidal shapes programmed into an interactive computer. Our conclusion on testing the method for a series of solids with known optical constants is that the method is a qualified success but could use some more refining and evaluation. It is clear that shape effects in the region of strong absorption are extremely important. Since every powder may have its own unique shape distribution it is difficult to construct a general theory of shape effects that works perfectly for all powders. The other side of this shape distribution sensitivity is that control of particle shape can markedly enhance peak extinction or broaden and widen the band. Understanding of these effects are important in the ultimate goal of being able to engineer the optical properties of particulate systems.

In future work it is suggested that more of the same kind of close comparison between optical constants determined from single crystals and from powders be carried out. Although most solids cannot be obtained as single crystals there are still quite a few silicate minerals that can be acquired as

- natural single crystals, whose optical constants have not been measured in the infrared. These silicates all have strong bands in the important 10 μm region because of their common Si-O vibrational bands. Measurement and cataloguing of such single crystal optical constants in the 5-15 μm region coupled with simultaneous efforts to extract optical constants from powders of the same materials will be pursued with support of next year's NASC contract.

REFERENCES

Carlon, H. R., 1979, Appl. Opt. 18, 1372.

Carlon, H. R., et. al., 1977, Appl. Opt. 16, 1598.

Churchill, R. V., 1960, Complex variables and applications, (McGraw-Hill:New York).

Day, K. L., Steyer, T. R., and Huffman, D. R., 1974, Ap. J. 191, 415.

Dorschner, J., Friedemann, C., and Gurtler, J., 1978, Astron. Nachr. 299, 269.

Gielisse, P. J., 1965, J. Appl. Phys. 36, 2446.

Hellwege, K. H., Lesch, W., Plihal, M., and Schaack, 1970, Z. Physik 232, 61.

Hodgson, J. N., 1970, Optical absorption and dispersion in solids, (Chapman and Hall:London).

Huffman, D. R., 1977, Ad. in Phys. 26, 129.

Huffman, D. R., and Bohren, C. F., 1979a, Proceedings of the international workshop on light scattering by irregularly shaped particles, June 5-7, 1979, Albany, N. Y., in press.

Huffman, D. R., and Bohren, C. F., 1979b, Proceedings of the workshop on artificial aerosols, Vail, Colo., June 19,20, 1797, in press.

van de Hulst, H. C., 1957, Light scattering by small particles, (Wiley:London).

Jennings, S. G., Pinnick, R. G., and Gillespie, J. B., 1979, Appl. Opt. 18, 1368.

McCrone, W. C., and Delly, J. G., 1973, The particle atlas, (Ann Arbor Science Pub.: Ann Arbor).

O'Conner, J. R., and Smiltens, J. eds., 1959, Silicon carbide, (Pergamon: New York).

Penman, J. M., 1976a, Mon. Not. R. astr. Soc. 176, 539.

Penman, J. M., 1976b, Mon. Not. R. Astr. Soc. 175, 149.

Perry, C. H. et. al., 1972, The Moon 4, 315.

Spitzer, W. G., and Kleinman, D. A., 1961, Phys. Rev. 121, 1324.

Spitzer, W. G., Kleinman, D., and Walsh, D., 1959, Phys. Rev. 113, 127.

Stern, F., 1964, Solid State Physics Vol. 15, ed. F. Seitz and D. Turnbull (Academic Press: New York).

Volz, F. E., 1972, Appl. Opt. 11, 755 (1972).